Clinical Neurophysiology 186 (2026) 2111860

Contents lists available at ScienceDirect

Clinical Neurophysiology

journal homepage: www.elsevier.com/locate/clinph

Enriched resting-state EEG prediction of cognitive decline in prodromal Alzheimer's disease: a machine-learning approach

Claudio Babiloni [a,b], Susanna Lopez [a,*], Giuseppe Noce [c], Claudio Del Percio [a], Roberta Lizio [a,d], Dharmendra Jakhar [a], Mina De Bartolo [a], Raffaele Ferri [d], Filippo Carducci [a,d], Valentina Catania [d], Andrea Soricelli [c,e], Marco Salvatore [c], Dario Arnaldi [f,g], Francesco Famà [f,g], Andrea Brugnolo [g,h], Matteo Pardini [g,h], Franco Giubilei [i], Fabrizio Stocchi [j,k], Laura Vacca [j], Chiara Coletti [j], Fabrizia D'Antonio [l], Giuseppe Bruno [l], Bahar Güntekin [m,n], Lutfu Hanoğlu [n,o], Harun Yırıkoğulları [n], Görsev Yener [p,q], Giacomo Russo [r], Moira Marizzoni [s], Giovanni B. Frisoni [t,u], Rossella Rotondo [b], Tiziana D'Alessandro [v], Nicole Dalia Cilia [w], Maria Francesca De Pandis [b,x], Adolfo Santoro [y], Simone Marziali [b], Claudio De Stefano [v], Francesco Fontanella [v]

[a] Department of Physiology and Pharmacology "Vittorio Erspamer," Sapienza University of Rome, Rome, Italy
[b] IRCCS San Raffaele Roma, Cassino Site Via G Di Biasio, 1, 03043 Cassino, FR, Italy
[c] IRCCS Synlab SDN, Naples, Italy
[d] Oasi Research Institute-IRCCS, Troina, Italy
[e] Department of Medical, Movement and Wellbeing Sciences, University of Naples Parthenope, Naples, Italy
[f] Neurofisiopatologia, IRCCS Ospedale Policlinico San Martino, Genova, Italy
[g] Clinica Neurologica, IRCCS Ospedale Policlinico San Martino, Genova, Italy
[h] Dipartimento di Neuroscienze, Oftalmologia, Genetica, Riabilitazione e Scienze Materno-infantili (DiNOGMI), Università di Genova, Italy
[i] Department of Neuroscience, Mental Health, and Sensory Organs, Sapienza University of Rome, Rome, Italy
[j] IRCCS San Raffaele, Rome, Italy
[k] Telematic University San Raffaele Rome, Rome, Italy
[l] Department of Human Neurosciences, Sapienza University of Rome, Rome, Italy
[m] Department of Biophysics, School of Medicine, Istanbul Medipol University, Istanbul, Turkey
[n] Research Institute for Health Sciences and Technologies (SABITA), Istanbul Medipol University, Istanbul, Turkey
[o] Department of Neurology, School of Medicine, Istanbul Medipol University, Istanbul, Turkey
[p] Department of Neurology, Faculty of Medicine, Dokuz Eylül University, 35340 İzmir, Turkey
[q] IBG: International Biomedicine and Genome Center, 35340 Izmir, Turkey
[r] SenTech Srl, Rome, Italy
[s] Biological Psychiatry Unit, IRCCS Istituto Centro San Giovanni di Dio Fatebenefratelli, 25125 Brescia, Italy
[t] Memory Clinic and LANVIE - Laboratory of Neuroimaging of Aging, University Hospitals and the University of Geneva, Geneva, Switzerland
[u] Geneva Memory Center, Department of Rehabilitation and Geriatrics, Geneva University Hospitals, Geneva, Switzerland
[v] Department of Electric and Information Engineering "Maurizio Scarano," University of Cassino and Southern Lazio, Cassino, Italy
[w] University of Enna "Kore," Enna, Italy
[x] Department of Human Science and Promotion of Quality of Life, San Raffaele Rome University 00166 Rome, Italy
[y] Natural Intelligent Technologies Srl., Italy

ARTICLE INFO

Keywords:
Alzheimer's disease (AD)
Mild cognitive impairment (MCI)
Biomarkers
Resting-state electroencephalographic (rsEEG) rhythms
Cerebro spinal fluid (CSF)

ABSTRACT

Objective: We evaluated the accuracy of standard machine learning (ML) algorithms in predicting 1-year cognitive decline in Alzheimer's disease patients with mild cognitive impairment (ADMCI) using resting-state electroencephalographic (rsEEG) biomarkers enriched with APOE genotype, sex, age, and educational attainment data.

Methods: The study analyzed datasets from 63 ADMCI patients obtained from an international archive. The ML algorithms included Simple Logistic Regression, Model Trees, Logistic Regression, K-nearest neighbor, and

* Corresponding author.
E-mail address: susanna.lopez@uniroma1.it (S. Lopez).

https://doi.org/10.1016/j.clinph.2026.2111860
Accepted 19 March 2026
Available online 25 March 2026

Delta, theta, and alpha rhythms
Structural Magnetic Resonance Imaging (sMRI)
Prediction
Artificial intelligence (AI)
Machine learning (ML)

Support Vector Machine. Input features comprised lobar rsEEG source activities across delta (<4 Hz) to alpha (≈10-12 Hz) bands, cerebrospinal fluid (CSF Aβ1-42/p-tau), and structural magnetic resonance imaging (sMRI) biomarkers. Cognitive decline was assessed over a 1-year follow-up ("stable" vs. "decliner") based on Mini-Mental State Examination (MMSE) scores.
Results: The four independent ML algorithms accurately predicted changes in the MMSE score over a 1-year follow-up, with accuracies of 77–78% in ADMCI participants aged ≥ 70 years and 74–77% in those aged < 70 years.
Conclusions and Significance.
These findings suggest that rsEEG biomarkers in ADMCI patients may not only reveal underlying pathophysiological mechanisms affecting cortical arousal and vigilance but also hold predictive value for cognitive outcomes.

1. Introduction

A panel of experts from the National Institute of Aging and Alzheimer's Association (AA-NIA) has recently updated (Jack et al., 2024) a well-known theoretical framework for the neurobiological diagnosis of Alzheimer's disease (AD) for research entitled "*Research Framework: Toward a biological definition of Alzheimer's Disease*" (Jack et al., 2018).

The update confirms the original statement that the AD diagnosis should be based on biomarkers of the neuropathology characterizing AD, derived from in to vivo measurement with fluid (cerebrospinal fluid, CSF, or blood plasma) or neuroimaging (positron emission tomography, PET) biomarkers (Jack et al., 2018). The neurobiological diagnosis of AD is based on a substantial accumulation of amyloidosis (A) and tauopathy (T) in the brain (Jack et al., 2018). Along the lines of the original thesis, the AD diagnosis would be made regardless of the disease's clinical manifestation (C) in the continuum from asymptomatic persons to subjective cognitive decline (ADSCD), mild cognitive impairment (MCI), and mild, moderate, or severe degree of dementia (ADD; Jack et al., 2018). In other words, for research purposes, investigators may formulate a diagnosis of AD even in older people with normal scores to the neuropsychological tests of cognitive functions if they are positive for CSF or PET biomarkers of amyloidosis (A) and tauopathy (T).

In the revised AA-NIA Framework (Jack et al., 2024), a key role continues to be played by biomarkers of brain neural degeneration (structural magnetic resonance imaging, sMRI, and fluid biomarkers). As a main novelty, the update extends the biomarkers of interest beyond the original A-T-N domain. It emphasized the importance of biomarkers non-specific for AD that enrich the prognosis, prediction, monitoring, and therapy response during the disease progression (Jack et al., 2024).

A promising integration of the A-T-N(C) Framework may be made with neurophysiological (Pathophysiological, P) biomarkers derived from the abnormal oscillations of the neurophysiological excitatory/inhibitory balance in the activity of the neural populations within and between encephalic regions and their relationship with the consciousness-vigilance levels from alertness to sleep (Babiloni et al., 2020a). Although these P biomarkers may be unspecific for AD-dependent neuropathology and neurodegeneration, they may be adopted to monitor and evaluate the effects of interventions against vigilance dysfunctions as non-cognitive symptoms. Indeed, this symptomatology may have a deleterious impact on the quality of a patient's life, being related to disabilities in watching TV news, reading newspapers, and maintaining quiet social conversation (Babiloni, 2022). The dysregulation of vigilance in AD patients is reflected by high levels of diurnal (morning) drowsiness (Bonanni et al., 2005; Brzecka et al., 2018; Moran et al., 2005; Peter-Derex et al., 2015), associated with cognitive deficits and other clinical manifestations (Lee et al., 2007).

These P biomarkers can be investigated by analyzing the ongoing electroencephalographic (EEG) or magnetoencephalographic (MEG) activity recorded during the resting-state eyes closed condition (Babiloni et al., 2020a). Specifically, the wakefulness-promoting systems in the brainstem, basal forebrain, hypothalamic, and thalamic-cortical loops do generate background high-voltage EEG activity at moderate frequencies (8–12 Hz) during quiet vigilance, while transient low-voltage EEG activity at high-frequencies (> 16 Hz) is produced during cognitive-motor events (Babiloni et al., 2020a).

But is EEG activity heuristically or neurophysiological relevant for assessing AD patients? To answer this question, ISTAART Electrophysiology Professional Interest Area (E-PIA) experts have recently reviewed the EEG-AD literature and reported the following outcome for the resting-state eyes-closed EEG (rsEEG) rhythms (Babiloni et al., 2020b, 2021a). Compared to control old individuals, AD patients showed the following effects: (1) higher rsEEG power density and interdependence between electrode or source pairs at delta (<4 Hz) and theta (4–7 Hz) frequency bands; (2) lower rsEEG power density and interdependence between electrode or source pairs at alpha (8–12 Hz) frequency band (as a sign of hyperexcitability) in posterior scalp regions; (3) > 80% accuracy of those rsEEG biomarkers in discriminating between ADMCI and ADD patients versus matched controls; (4) increased abnormalities in rsEEG power density and interdependence between electrode or source pairs at 12–24-month follow-ups and some signs of beneficial effects during 6–24-month intervention trials using standard symptomatic cholinergic drugs (Babiloni et al., 2020a,b, 2021a). In parallel, a similar outcome was reported by experts from the International Federation of Clinical Neurophysiology (Rossini et al., 2020). These rsEEG results indicate a dysregulation of the neurophysiological mechanisms underpinning vigilance maintenance in AD patients at both group and individual levels.

Previous longitudinal studies also evaluated the value of rsEEG biomarkers in predicting cognitive decline in AD patients at follow-ups. The results can be summarized as follows: (1) combined rsEEG alpha and theta power density and mean frequency from left temporal-occipital regions predicted cognitive decline in ADMCI patients at about 1-year follow-up (Jelic et al., 2000); (2) high temporal rsEEG delta source activity predicted marked cognitive decline in ADMCI patients at an average of about 1-year follow-up (Rossini et al., 2006); (3) low posterior rsEEG alpha power density predicted the cognitive decline in ADMCI and ADD patients at about 1-year follow-up (Luckhaus et al., 2008); (4) high rsEEG delta-theta and lower rsEEG alpha power density predicted clinical worsening > 1 year in patients with ADSCD and ADMCI (Gouw et al., 2017); (5) anterior localization of rsEEG alpha sources predicted the cognitive decline in ADMCI patients at about 2-year follow-up (Huang et al., 2000); (6) baseline high rsEEG theta power density and cognitive performance predicted cognitive decline at about 2-year follow-up with an overall predictive accuracy of 93% in persons ranging from intact cognition to ADMCI and ADD conditions (Nobili et al., 1999; Babiloni et al., 2014); (7) ADMCI patients with high- and low-frequency rsEEG alpha frequency power density ratio at scalp electrodes presented greater cortical atrophy and lower perfusion rate in the temporo-parietal cortex as revealed by neuroimaging markers and conversion to ADD status at about 3-year follow-up (Moretti, 2015); an (8) high temporoparietal rsEEG theta power density and slowing of mean rsEEG frequency predicted cognitive decline from SCD to significant cognitive deficits at about 7–9-year follow-ups with an overall predictive accuracy of 90%, thus extending previous evidence of the same Workgroup in healthy, SCD, ADMCI, and ADD individuals (Prichep et al., 1994, 2006, 2014).

Overall, the above studies showed converging findings showing that rsEEG delta, theta, and alpha rhythms were abnormal in AD patients

evaluated at several disease stages (Babiloni et al., 2020b, 2021a). Furthermore, the quantitative analysis of those rhythms could monitor and predict cognitive decline even at a relatively short follow-up of 1 year (Babiloni et al., 2020b, 2021a, 2024; Niu et al., 2024). These changes were interpreted as an abnormal synchronization at slow frequencies (< 7 Hz) of the activity of cortical pyramidal neurons triggered by neurons of the thalamocortical and corticothalamic circuits that show bursting of action potentials at these slow frequencies (Jeanmonod et al., 1996; Llinás and Steriade, 2006). This bursting mode would inhibit information processing in thalamocortical and corticothalamic neurons for the relatively long interval of membrane hyperpolarization (inhibition) between two action potential bursts (Llinás and Steriade, 2006). Therefore, there would be a derangement of the functional connectivity involving the cholinergic basal forebrain, thalamic, and visual cortical networks from the early disease stages (Lopez et al., 2024).

Clinical applications of rsEEG biomarkers are hindered by their complex interactions with age (Babiloni et al., 2021b), sex (Babiloni et al., 2022), and educational attainment (Babiloni et al., 2021c), which should be considered when interpreting rsEEG results. Specifically, posterior rsEEG alpha rhythms have been found to be lower in the younger than the older ADMCI subgroup, suggesting a greater disease aggressivity in the former than in the latter (Babiloni et al., 2021b). These rhythms were also lower in the male than in the female ADMCI subgroup (Babiloni et al., 2021b), pointing to possible protective effects of sexual hormones. The same effect was observed in the ADMCI subgroup with higher educational attainment compared to lower educational attainment (Babiloni et al., 2021c), revealing a compensatory effect of this proxy for cognitive reserve.

Another significant issue is whether the comparative predictive value of those rsEEG biomarkers aligns with the standard A-T-N biomarkers of the mentioned Framework (Jack et al., 2018). For example, previous sMRI evidence pointed to steeper medial lobe atrophy with age in ADMCI and ADD patients than in normal older seniors without cognitive deficits (Nolder) (Rhodius-Meester et al., 2017). Previous sMRI evidence also suggested that aging and AD have an aging effect on gray matter atrophy in several other brain regions (Pichet Binette et al., 2020). In ADMCI patients, a similarly addictive effect of age and AD was observed on CSF biomarkers of neuropathology and MRI biomarkers of the default mode cortical network and white matter microstructure (Brown et al., 2018).

The present retrospective study evaluated the accuracy of artificial intelligence—machine learning (ML) tools in predicting cognitive decline in ADMCI patients at 1-year follow-ups, based on rsEEG source activity enriched by APOE genotyping, sex, age, and education attainment information typically available during clinical assessment of those patients. The results were compared to those obtained with the enriched CSF and sMRI biomarkers of the A-T-N(C) Framework (Jack et al., 2018).

The clinical and instrumental (rsEEG, sMRI, and CSF) datasets were taken from two international archives of The PDWAVES Consortium (www.pharmacog.eu) and PharmaCog (https://www.imi.europa.eu/projects-results/project-factsheets/pharma-cog). The prediction was based on four independent ML tools, such as Simple Logistic Regression Model Trees (Breiman et al., 1984; Friedman et al., 2000), Logistic Regression (Fletcher, 1987; Yu et al., 2011), K-Nearest Neighbor (Bishop, 2006), and Support Vector Machine (Chang and Lin, 2011). The output performances of the four ML tools were averaged as an index of prediction accuracy. The target cognitive status ("stable" vs. "decliner") at 1-year follow-ups of the ADMCI individuals patients' global cognitive status in memory clinics worldwide. As "early" and "late" onsets of AD are associated with different clinical presentations and brain abnormalities (Licht et al., 2007; Seath et al., 2023; Wattmo et al., 2017; Babiloni et al., 2021b), we stratified the ADMCI patients into two groups substantially matched as numerosity, sex, and education attainment: the group of ADMCI patients having < 70 years and that of ADMCI patients having ≥ 70 years.

2. Materials and methods

2.1. Participants and diagnostic criteria

The Partners and institutional affiliations of the PDWAVES Consortium and the PharmaCog project are reported on the cover page of this manuscript. The datasets used were formed by clinical, neuropsychological, anthropometric, genetic, CSF, sMRI, and rsEEG markers obtained in 63 ADMCI patients (mean age: 69.7 ± 0.8 standard error of the mean, SE, years; age range: 56–81 years 30 male; mean education: 10.7 ± 0.5 SE years; MMSE score: 25.2 ± 0.3 SE) and 60 Nolder seniors as controls (mean age: 69.5 ± 0.8 SE years; age range: 52–81 years 27 male; mean education: 10.3 ± 0.5 SE years; MMSE, score: 28.5 ± 0.1 SE). The ADMCI and Nolder groups were carefully matched for age, gender, and education. Statistical analyses ($p < 0.05$) were performed to evaluate the presence or absence of statistically significant differences ($p < 0.05$) between the two groups for the age (*T*-test), gender (Fisher test), educational attainment (*T*-test), and MMSE score (Mann Whitney *U* test). As expected, a statistically significant difference was found for the MMSE score ($p < 0.00001$), showing a higher score in the Nolder than in the ADMCI group. On the contrary, no statistically significant differences were found in the age, gender, and educational attainment between the groups ($p > 0.05$).

These Nolder and ADMCI participants were recruited by the following Italian and Turkish clinical units of the PDWAVES Consortium: the Sapienza University of Rome (Italy), the Institute for Research and Evidence-based Care (IRCCS) "Fatebenefratelli" of Brescia (Italy), the IRCCS Synlab SDN of Naples (Italy), the Oasi Research Institute-IRCCS, Troina (Italy), the IRCCS Ospedale Policlinico San Martino and DINOGMI (University of Genova, Italy), the Hospital San Raffaele of Cassino (Italy), the IRCCS San Raffaele Pisana of Rome (Italy), the Izmir University of Economics, Faculty of Medicine (Turkey), and the Medipol University of Istanbul (Turkey).

Local institutional Ethics Committees approved the present observational study. All experiments were performed with each participant's overt consent, in line with the Code of Ethics of the World Medical Association (Declaration of Helsinki) and the standards established by the local Institutional Review Board.

The diagnosis of AD in the ADMCI patients was based on the "positivity" to Aβ1-42/phospho-tau ratio (Aβ42/p-tau) in the CSF biomarker or MRI evidence of neurodegeneration in the typical neuroanatomical targets of the disease in the hippocampus, temporoparietal junction, precuneus, and posterior cingulate regions (Albert et al., 2011). The physicians in charge judged the "positivity" for releasing the clinical diagnosis of "AD" to the patients, according to the local diagnostic routine of the participating clinical Units.

The clinical inclusion criteria of the ADMCI patients were as follows: (1) age of 55–90 years; (2) reported memory complaints by the patient and a relative; (3) MMSE score of 24 or higher; (4) Clinical Dementia Rating (CDR) score of 0.5 (Morris, 1993); (5) logical or verbal memory test score of 1.5 standard deviations (SD) below the mean adjusted for age (Rey, 1968; Wechsler, 1987); the cognitive deficits did not have to significantly interfere with the functional independence in the activities of the daily living; (6) Geriatric Depression Scale (15-item GDS; Brown and Schinka, 2005) score of 5 or lower; (7) modified Hachinski ischemia (Rosen et al., 1980) score of 4 or lower and education of 5 years or higher; and (8) single or multi-domain amnesic MCI status.

The clinical exclusion criteria of the ADMCI patients were as follows: (1) other significant systemic, psychiatric, and neurological illness; (2) any form of dementia or mixed dementia; (3) actual participation in a clinical trial using disease-modifying drugs; (4) systematic use of antidepressant drugs with anticholinergic side effects; (5) chronic use of neuroleptics, narcotics, analgesics, sedatives or hypnotics; (6) and antiparkinsonian medications (cholinesterase inhibitors and memantine allowed); (7) diagnosis of epilepsy or report of seizures or epileptiform EEG signatures in the past, and (8) major depression disorders described

in the Diagnostic and Statistical Manual of Mental Disorders (DSM-5).

In all ADMCI patients, AD-relevant CSF biomarkers were assessed in a neurobiological definition of AD in line with the NIA-AA Research Framework (Albert et al., 2011; Jack et al., 2018). The CSF samples were preprocessed, frozen, and stored in line with the Alzheimer's Association Quality Control Programme for CSF biomarkers (Mattsson, 2011). Dedicated single-parameter colorimetric enzyme-linked immunosorbent assay ELISA kits (Innogenetics, Ghent, Belgium) were used to measure amyloid beta 1–42 (i.e., Aβ42). Levels of the protein tau (i.e., total tau, t-tau) and a phosphorylated form of tau at residue 181 (i.e., p-tau) were also measured. From one frozen aliquot of CSF, the assays were run parallel according to the manufacturer's instructions. Each sample was assessed in duplicate. A sigmoidal standard curve was plotted to allow the quantitative expression (pg mL^{-1}) of measured light absorbance. All ADMCI patients of the present study were "positive" for the CSF Aβ42/p-tau biomarker with a threshold defined in a previous investigation of our Workgroup (Marizzoni et al., 2020). In that investigation, the cut-off of "positivity" to that CSF Aβ42/p-tau biomarker was 15.2 for *APOE* ε4 (*APOE4)* carriers and 8.9 for *APOE4* non-carriers (Marizzoni et al., 2020). In the present study, all ADMCI patients with *APOE4* status had CSF Aβ42/p-tau lower than 15.2, whereas the ADMCI patients without *APOE* status had CSF Aβ42/p-tau lower than 8.9.

Furthermore, in all ADMCI patients, relevant sMRI markers were measured. All sMRI scans were performed using 3.0 Tesla machines. The sMRI protocol consisted of several acquisitions, including two T1-weighted, anatomical T2-weighted/FLAIR, fluid-attenuated inversion recovery (FLAIR), and diffusion tensor imaging scans. Only anatomical T1-weighted/FLAIR scans were available for all units and were analyzed in the present study.

In the centralized analysis of the sMRIs, all data were visually inspected for quality assurance before extracting the MRI biomarkers. Specifically, we checked that there were no gross partial brain coverage errors or major visible artifacts, including motion, wrap-around, radio frequency interference, and signal intensity or contrast inhomogeneities. The two anatomical T1-weighted sMRI scans were averaged. The data were analyzed using FreeSurfer version 5.1.0 to automatically generate: (1) volumes of the total gray matter, total white matter, caudate nucleus, putamen nucleus, pallidum nucleus, accumbens nucleus, hippocampus, amygdala, and lateral ventricle; (2) total cortical thicknesses of the entorhinal cortex; and (3) white matter hypointensity (Fischl et al., 2004; Desikan et al., 2006). Those volumes were normalized to the total intracranial volume (TIV). Furthermore, the T2-weighted FLAIR MRI scans were analyzed using the FMRIB Software Library (FSL) version 5.0.3 to evaluate the subcortical white matter lesions to control for the AD diagnosis.

Furthermore, *APOE* genotyping, anthropometric features (i.e., weight, height, and body mass index), and cardiocirculatory markers (i.e., systolic pressure, diastolic pressure, pulse pressure, mean arterial pressure, and heart frequency) were also measured as control variables for diagnostic purposes.

In all ADMCI patients, the global cognitive status and performance in various cognitive domains, including memory, language, executive function, planning, visuospatial function, and attention, were assessed. All ADMCI patients showed a significant reduction in performance in at least one episodic memory test, in most cases associated with a significant reduction in the performance at neuropsychological tests probing other cognitive domains. In the following, we report the cognitive domains explored and the neuropsychological tests administered to the ADMCI patients: (1) the global cognitive status was tested by the MMSE and the Alzheimer's Disease Assessment Scale–Cognitive Subscale (ADAS-Cog; Rosen et al., 1984; Folstein et al., 1975); (2) the episodic memory was assessed by the immediate and delayed recall of the Rey Auditory Verbal Learning Test (Rey, 1968); (3) the executive functions and attention were evaluated by the Trail making test (TMT) parts A and B (Reitan, 1958); (4) the language was tested by 1-min Verbal fluency test for letters and 1-min Verbal fluency test for category (fruits, animals or car trades) (Novelli et al., 1986); and (5) planning abilities and visuospatial functions were assessed by the Clock drawing and copy test (Freedman et al., 1994).

All Nolder seniors underwent an interview and cognitive screening (including MMSE and GDS) and physical and neurological examinations to exclude subjective memory complaints (SMC), cognitive deficits, and mood disorders. All Nolder seniors had an MMSE score $\geq$ 27, a CDR score equal to 0, and a GDS score lower than the threshold of 5 (no depression) or were evaluated as having no depression after an interview with a physician or clinical psychologist at the time of the enrolment. The Nolder seniors with a history of previous or present neurological or psychiatric disease were also excluded. Furthermore, the Nolder seniors affected by any chronic systemic illnesses (e.g., diabetes mellitus) were excluded, as were the Nolder seniors taking chronically psychoactive drugs. Unfortunately, sMRI, CSF, and *APOE* genotyping were unavailable for the present Nolder seniors.

Table 1 reports the relevant demographic and clinical information (i.e., MMSE score) about the Nolder and ADMCI groups, together with the results of the statistical analyses computed to evaluate the presence or absence of statistically significant differences among them as age (*t*-test), sex/gender (Fisher's exact test), education (*t*-test), and MMSE score (Mann-Whitney *U* test). As expected, a statistically significant difference was found between the two groups for the MMSE score ($p = 0.00001$), showing a higher score in the Nolder than in the ADMCI group. On the contrary, we observed no statistically significant differences in age, gender, and education between the groups ($p > 0.05$).

Table 2 reports the additional clinical, genetic, and CSF data relevant to characterize the ADMCI group for future cross-validation studies. Specifically, the mean scores (± SE) of GDS, CDR, and modified Hachinski ischemia test are reported. The mean percentage of *APOE* genetic risk for AD and the mean group values of CSF p-tau (pg/ml), t-tau (pg/ml), and Aβ42/p-tau diagnostic biomarkers for AD are also reported.

2.2. The resting state electroencephalographic (rsEEG) recordings

The rsEEG activity was recorded while the participants were relaxed with eyes closed and seated on a comfortable reclined chair in a silent room with dim lights. Instructions encouraged the participants to experience quiet wakefulness with muscle relaxation, no voluntary movements, no talking, and no development of systematic goal-oriented mentalization during the rsEEG recording. Rather, a quiet, wondering mode of mentalization was kindly required. The participants, including the ADMCI patients, did not experience any significant difficulties following those instructions.

All participants' (eyes-closed) rsEEG recordings lasted about 3–5 min. Considering all clinical recording units, the rsEEG data were

Table 1
Relevant demographic and clinical information from patients with Alzheimer's disease at the prodromal clinical stage of amnesic mild cognitive impairment (ADMCI) and cognitively unimpaired normal old (Nolder) seniors. The table also reports the results of the statistical analyses ($p < 0.05$ uncorrected) computed to evaluate the presence or absence of statistically significant differences among the Nolder and ADMCI groups as age (*t*-test), sex (Male/Female; Fisher's exact test), educational attainment (*t*-test), and MMSE score (Mann-Whitney *U* test). Legend: MMSE = mini-mental state evaluation; n.s. = not significant.

Demographic and clinical data in the Nolder and ADMCI persons			
	Nolder	**ADMCI**	**Statistical analysis**
N	57	63	
Age (years)	69.6 ± 0.8 SE	69.6 ± 0.8 SE	T-test: n.s.
Sex (M/F)	26/31	24/39	Fisher test: n.s.
Education (years)	10.4 ± 0.5 SE	11.3 ± 0.6 SE	T-test: n.s.
MMSE score	28.5 ± 0.1 SE	26.3 ± 0.2 SE	Mann-Whitney *U* test: $p < 0.00001$

Table 2
Mean (± standard error of the mean, SE) values of the clinical, genetic (percentage of apolipoprotein E epsilon 4 carriers), and cerebrospinal fluid markers obtained in the ADMCI patients of the present study. The cerebrospinal fluid (CSF) markers include phospho-tau (p-tau; pg/ml), total-tau (t-tau; pg/ml), and the ratio between amyloid beta 1–42 and phospho-tau (Aβ1-42/p-tau).

Clinical, genetic (*APOE*), and cerebrospinal fluid markers in the ADMCI patients	
Clinical markers	
Geriatric depression scale	2.6 ± 0.3 SE
Clinical dementia rating	0.5 ± 0.0 SE
Hachinski ischemic score	0.9 ± 0.1 SE
Genetic marker	
APOE4 (%)	67.4%
Cerebrospinal fluid markers	
Aβ1-42 (pg/ml)	493 ± 22 SE
p-tau (pg/ml)	77 ± 5 SE
t-tau (pg/ml)	549 ± 44 SE
Aβ1-42/p-tau	7 ± 1 SE

recorded with a 128–512 Hz sampling frequency and related antialiasing band passes between 0.01 Hz and 60–100 Hz. The electrode montage included 19 scalp monopolar sensors placed following the 10–20 System (i.e., O1, O2, P3, Pz, P4, T3, T5, T4, T6, C3, Cz, C4, F7, F3, Fz, F4, F8, Fp1, and Fp2). A frontal ground electrode was used, while cephalic or linked earlobe electrodes were used as electric references according to local methodological facilities and standards. Electrode impedances were kept below 5 kΩ. Vertical and horizontal electro-oculographic (EOG) potentials (0.3–70 Hz bandpass) were recorded to control eye movements and blinking.

2.3. The preliminary rsEEG data analysis

The preliminary analysis of the recorded rsEEG activity followed the same procedures of previous rsEEG investigations performed in ADMCI patients by the PDWAVES Consortium (Babiloni et al., 2017, 2018) to compare the results across the various studies.

For this analysis, the rsEEG data were re-sampled to a sampling frequency of 128 Hz, divided into epochs of 2 s, and analyzed offline.

The rsEEG epochs affected by any physiological (ocular/ blinking, muscular, cardiac, and head movements) or non-physiological (sweat, bad contact between electrodes and scalp, etc.) artifacts were identified and discarded by the visual analysis of two experts of EEG signals (C.D. P., G.N., or S.L.). In this visual analysis, the contamination of rsEEG rhythms with the ocular activity or blinking was mainly evaluated in the frontal electrodes (i.e., F7, F3, Fz, F4, F8, Fp1, and Fp2), comparing the EOG and EEG traces. Head movement artifacts were detected based on typical features, such as a sudden and great amplitude increase in slow EEG waves in all scalp electrodes. Muscle tension artifacts were recognized by observing the effects of several frequency bandpass filters in different ranges and examining the rsEEG power density spectra. These artifacts were reflected by unusually high and stable values of rsEEG power density from 30 to 60 Hz, which contrast with the typical declining trend of rsEEG power density from 25 Hz onward in artifact-free EEG traces. The experimenters also detected rsEEG epochs with signs of sleep intrusion (even if the rsEEG recordings lasted few minutes), such as progressive amplitude increase of frontal theta rhythms, followed by K complexes, sleep spindles, vertex shape waves, and slow waves. Furthermore, the two experimenters carefully rejected rsEEG epochs associated with behavioral annotations taken during the experiments (e.g., report of participant's drowsiness, opened eyes, arm/hand movements, or experimenter's verbal warnings, etc.).

As a result of the above procedures, the artifact-free rsEEG epochs showed the same proportion of the total rsEEG activity recorded in the Nolder and ADMCI groups (> 80%). In particular, the mean of artifact-free rsEEG epochs were 130 (± 3 SE; 88%) in the Nolder group and 128 (± 4 SE; 86%) in the ADMCI group. An ANOVA with the factor Group (Nolder and ADMCI) showed no statistically significant difference ($p > 0.05$) in the amount of artifact-free rsEEG epochs. The mean lengthiness of the artifact-free rsEEG activity was about 4 min for each group, ensuring the reliability of the rsEEG alpha power density (Salinsky et al., 1991; Babiloni et al., 2018).

2.4. The scalp power density of rsEEG rhythms

For each ADMCI and Nolder participant, the global normalized rsEEG power density at the scalp electrode level was evaluated. In detail, the procedure was performed as follows: (1) a standard digital FFT-based power spectrum analysis (Welch technique, Hanning windowing function, no phase shift) computed the absolute scalp power density of rsEEG rhythms with 0.5 Hz of frequency resolution at each electrode (i.e., 19 electrodes of the 10–20 montage system) and frequency bin (i.e., 0.5–45 Hz) from all artifact-free rsEEG epochs; (2) the scalp rsEEG power density at each electrode and frequency bin was normalized to the mean value obtained by averaging the scalp rsEEG power density across all frequency bins and scalp electrodes; (3) The "global" scalp normalized rsEEG power density at each frequency bin was calculated by averaging the normalized scalp rsEEG power density values across all 19 electrodes of the 10–20 montage system; (4) The global scalp normalized rsEEG power density values at each frequency band of interest were averaged to obtain the frequency band values.

The rsEEG frequency bands of interest were individually identified based on the following frequency landmarks: rsEEG transition frequency (TF) and individual alpha frequency peak (IAFp; Klimesch, 1999, 2012). In the rsEEG power density spectrum, the TF marks the transition frequency between the theta and alpha bands, defined as the minimum rsEEG power density between 3 and 8 Hz (between the delta and the alpha power peak). The IAFp is the maximum rsEEG power density peak between 6 and 14 Hz. These frequency landmarks were previously well described by Dr. Wolfgang Klimesch (Klimesch et al., 1996; Klimesch et al., 1998). TF and IAFp were computed for each subject involved in the study. Based on the TF and IAFp, we estimated the individual rsEEG delta, theta, and alpha bands as follows: delta from TF −4 Hz to TF −2 Hz, theta from TF −2 Hz to TF, alpha 1 from TF to the frequency midpoint of the TF-IAFp range, alpha 2 from the frequency midpoint of the TF-IAFp range to IAFp, and alpha 3 IAFp to IAFp + 2 Hz.

The other bands with higher frequencies (beta and gamma) were not considered for the present study, based on the results obtained by the research group applying the present rsEEG methodological approach in the ADMCI patients (Babiloni et al., 2021b, Babiloni et al., 2021c; Babiloni et al., 2022).

2.5. The estimation of rsEEG cortical sources by low-resolution brain electromagnetic tomography (eLORETA) freeware

We used the official freeware tool, exact low-resolution brain electromagnetic tomography (eLORETA; https://www.uzh.ch/keyinst/loreta.htm), to linearly estimate the cortical source activity generating scalp-recorded rsEEG rhythms (Pascual-Marqui, 2007). The present implementation of eLORETA uses a realistic head volume conductor model composed of the scalp, skull, and brain. Exploring electrodes can be virtually positioned in the scalp compartment to give EEG data as an input to the source estimation (Pascual-Marqui, 2007). These compartments of the head model are based on a template used in many neuroimaging studies, namely that of the Montreal Neurological Institute (i.e., the MNI152 template).

The input for eLORETA source estimation is formed by the artifact-free EEG epochs with 19 scalp electrodes placed according to the 10–20 montage system. The output is the set of estimates of neural ionic currents in the equivalent current dipoles located in the 6,239 voxels with 5 mm resolution, restricted to the cortical gray matter of the realistic head volume conductor model. In that cortical source space, an equivalent current dipole is in each voxel. The eLORETA package

provides each voxel's Talairach coordinates, the cortical lobe, and the Brodmann area (BA).

The eLORETA freeware solves the so-called regularized EEG linear inverse problem, estimating "neural" current density values at any cortical voxel of the mentioned realistic head volume conductor model. The solutions are computed at all rsEEG frequency bin-by-frequency bin (0.5 Hz as frequency resolution, namely, the maximum frequency resolution allowed using 2-s artifact-free EEG epochs).

A regional analysis of the eLORETA solutions was performed in the following lobar macro-regions of interest (ROIs): frontal (Brodmann area, BA 8, 9, 10, 11, 44, 45, 46, and 47), central (BA 1, 2, 3, 4, and 6), parietal (BA 5, 7, 30, 39, 40, and 43), occipital (BA 17, 18, and 19), temporal (BA 20, 21, 22, 37, 38, 41, and 42), and limbic (BA 31, 32, 33, 34, 35, 36). The eLORETA solution for each of these lobar ROIs was obtained by the average of the normalized eLORETA current density values estimated at all single voxels included. For example, the eLORETA solution for the temporal ROI was obtained by the average of the normalized eLORETA current density values estimated at all voxels included in the BA 20, 21, 22, 37, 38, 41, and 42 of the bilateral temporal lobes.

An ANOVA evaluated the hypothesis that the eLORETA rsEEG source activities (i.e., regional normalized eLORETA current densities) may differ between the Nolder and ADMCI groups as a characterization of the ADMCI group for future cross-validation studies and to select the rsEEG source activities to be used to train the ML tools for the clinical prediction purposes in the ADMCI patients. The ANOVA factors were Group (Nolder and ADMCI), Band (delta, theta, alpha 2, and alpha 3), and ROI (frontal, central, parietal, occipital, temporal, and limbic). Mauchly's test evaluated the sphericity assumption, and the degrees of freedom were corrected by the Greenhouse-Geisser procedure when appropriate ($p < 0.05$). Duncan test was used for post-hoc comparisons ($p < 0.05$, corrected for multiple comparisons as explained in the following).

The results of the subsequent post-hoc statistical analyses were controlled by the iterative (leave-one-out) Grubbs' test, which detected the presence of one or more outliers in the distribution of the global scalp normalized rsEEG power densities and regional normalized eLORETA current densities of interest. The null hypothesis of the non-outlier status was evaluated at the arbitrary threshold of $p > 0.001$ to remove only individual values with a high probability of being outliers.

Fig. 1 shows an overview methodology used to estimate the cortical sources of rsEEG rhythms in ADMCI patients and Nolder participants.

2.6. *Artificial intelligence (AI) tools of machine learning for predicting the cognitive decline in patients with Alzheimer's disease mild cognitive impairment (ADMCI)*

As mentioned in an introductory section, we used the following four independent AI tools of machine learning to explore the performance of the enriched CSF, rsEEG, and sMRI biomarkers to predict the cognitive decline in ADMCI patients at 1-year follow-ups: Simple Logistic Regression Model Trees (Breiman et al., 1984; Friedman et al., 2000; Landwehr et al., 2005), Machine Learning Prediction with Logistic Regression (Fletcher, 1987; Yu et al., 2011), Machine Learning Prediction with K-Nearest Neighbor (Bishop, 2006), and Machine Learning Prediction with Support Vector Machine (Chang and Lin, 2011).

2.7. *Simple Logistic regression model Trees (SLO)*

Simple Logistic regression Model Trees (SLO) were shown to be accurate and compact classifiers (Landwehr et al., 2005). Indeed, SLO performs competitively with classifiers, such as boosted decision trees, while being easier to interpret (Landwehr et al., 2005). The cost of building the logistic regression models is performed at the nodes. The LogitBoost algorithm repeatedly calls for a fixed number of iterations, determined by a five-fold cross-validation (Friedman et al., 2000). SLO combines two complementary classification schemes: linear logistic

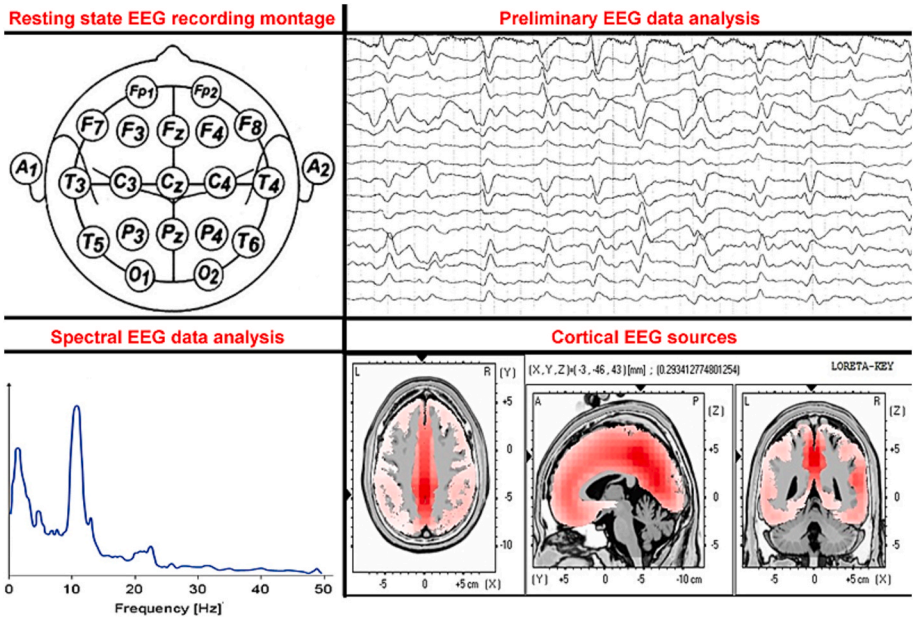

Fig. 1. An overview methodology used to estimate the cortical sources of resting-state eyes-closed electroencephalographic (rsEEG) rhythms in patients with Alzheimer's disease at the prodromal stage of amnesic mild cognitive impairment (ADMCI). Top (left): Diagram showing the placement of the 19 scalp electrodes of 10–20 International System adopted for the acquisition of rsEEG activity. (Right) Example of the rsEEG activity with ample ocular and blinking artifacts to be detected and removed by experts and a mathematical procedure based on independent component analysis. Bottom (left): an example of the rsEEG power density spectrum computed from the rsEEG activity recorded at an occipital electrode (i.e., O1) in a healthy old participant. (Right): an example of the cortical source solutions estimated from rsEEG alpha rhythms by the freeware called exact low-resolution brain electromagnetic tomography (eLORETA; https://www.uzh.ch/keyinst/loreta.htm) (https://www.uzh.ch/keyinst/loreta.htm). The eLORETA source solutions were averaged within cortical lobes and compared among groups of healthy old participants with unimpaired cognitive status (Nolder) and ADMCI patients. *Legend: rsEEG = resting-state eyes-closed electroencephalographic; ADMCI = Alzheimer's disease at the prodromal stage of amnesic mild cognitive impairment.*

regression and tree induction.

The linear logistic regression models the posterior class probabilities P r(G = j|X = x) for the J classes via functions linear in x, ensuring that they sum to one and remain in [0, 1]. The model is of the following form:

$$Pr(G = j|X = x) = \frac{e^{F_j(x)}}{\sum_{k=1}^{J} e^{F_k(x)}},$$

where Fj (x) = βT j · x. Numeric optimization algorithms that approach the maximum likelihood solution iteratively are used to find the estimates for βj. One of the typical iterative methods used is the LogitBoost algorithm (Friedman et al., 2000).

2.8. Logistic regression (LOG)

Logistic regression (LOG) is a linear classification algorithm that uses the logistic function to model class probabilities (Yu et al., 2011). Given a training set of instance-label pairs (**xi**, *yi*) *i* = …, *N*, where **x***i* ∈ R*M* and *yi* ∈ {1,−1}, LR requires the solution of the following optimization problem:

$$\min_{w,c} \frac{1}{2} w^T w + C \sum_{i=1}^{N} log\left(exp\left(-y_i\left(x_i^T w + c\right)\right) + 1\right)$$

To solve this problem, we used the lbfgs method. It approximates the Broyden–Fletcher–Goldfarb–Shanno algorithm (Fletcher, 1987), and it is an iterative method for solving unconstrained nonlinear optimization problems recommended for small datasets.

2.9. Machine learning prediction with k-nearest Neighbor (3-NN)

The K-nearest neighbor algorithm (3-NN) is a well-known nonparametric method that can be used for classification and regression (Bishop, 2006). According to this approach, an unknown sample is labeled with the most common label among its k nearest neighbors in the training set. The rationale behind the k-NN classifier is that, given an unknown sample **x** to be assigned to one of the c*i* classes of the problem at hand, the a-posteriori probabilities (c*i* |**x**) of **x** may be estimated as follows:

$$(ci|x) = ni/K$$

where *ni* is the number of samples among the *K* nearest neighbor of **x** belonging to the *ith* class.

2.10. Support Vector Machine (SVM)

Support Vector Machines (SVMs) are supervised learning methods based on the concept of decision planes (Chang and Lin, 2011). These planes are linearly separate (in the feature space) objects belonging to different classes. Intuitively, given two classes to be discriminated in each feature space, a good separation is achieved by the hyperplanes with the largest distance to the nearest training points belonging to different classes; in general, the larger the margin, the lower the generalization error of the classifier.

While the basic idea of the SVM applies to linear classifiers, they can be easily adapted to non-linear classification tasks using the so-called "kernel trick,' which implies mapping the original features into a higher dimensional feature space. Given a training set of instance-label pairs =

$$\min_{w,b,\xi} \frac{1}{2} w^T w + C \sum_{i=1}^{N} \xi_i$$

subject to *yi* (**w***T*ϕ(**x***i*) + *b*) ≥ 1 − ξ*i*, ξ*i* ≥ 0.

According to the above formulation, training samples are mapped into a higher dimensional space by the function ϕ. SVM finds a linear separating hyperplane with the maximal margin in this higher dimensional space. *C* > 0 is the penalty parameter of the error term. Furthermore, (**x***i*, **x***j*) ≡ (**x***i*) *T*(**x***i*) is called the kernel function. Typical kernels are:

linear: *K*(**x***i*, **x***j*) = **x** *Ti* **x***j*.

polynomial: *K*(**x***i*, **x***j*) = (γ**x** *Ti* $\mathbf{x}_j$ +*r*)^d, γ > 0.

γ > 0.

Where γ, *r*, and d are the kernel parameters.

Experimental design for the predictions with SLO, LOG, 3-NN, and SVM.

We used the following runs of input features for each AI tool separately (i.e., SLO, LOG, 3-NN, and SVM).

(1) ***CSF***: *APOE genotyping* status (carrier, non-carrier), CSF p-tau (pg/ml), t-tau (pg/ml), and Aβ42/p-tau, age, sex, education attainment.

(2) ***RsEEG***: Based on the results obtained using the present methodological approach in the ADMCI patients (Babiloni et al., 2021b, Babiloni et al., 2021c; Babiloni et al., 2022), rsEEG the features were individual parietal, temporal, and occipital delta sources; parietal, temporal, and occipital theta sources; parietal, temporal, and occipital alpha 2 sources; parietal, temporal, and occipital alpha 3 sources; parietal delta/alpha 2, occipital delta/alpha 2, parietal theta/alpha 2, and occipital theta/alpha 2 sources.

(3) ***T1-weighted sMRI***: global markers (white matter and gray matter volumes normalized for the total intracranial volume, total cortical thickness); ventricular markers (lateral ventricle volume normalized for the total intracranial volume); vascular lesion markers (subcortical white matter hypointensity); mesial temporal lobe markers (hippocampus and amygdala volumes normalized for the total intracranial volume; entorhinal thickness); basal ganglia markers (caudate nucleus, putamen nucleus, pallidum nucleus, and accumbens nucleus normalized for the total intracranial volume).

(4) ***ALL***: all the features reported in (1), (2), and (3) together as a gold standard. Each input feature (demographic, rsEEG, sMRI, and CSF) was rescaled from 0 (the minimum value of that feature along all the ADMCI patients) to 1 (the maximum feature value).

The AI tools were tested to predict the cognitive status of the ADMCI patients at 1-year follow-ups. Each ADMCI individual was defined as "stable" or "decliner" based on the difference in the MMSE score baseline minus 1-year follow-up. Specifically, we repeated the ML experiments three times based on the following extended definition of clinically "stable" or "decliner":

- First definition as "stable" if the difference in the MMSE score between baseline and 1-year follow-up was ≥ 0. Definition as "decliner" if that difference was < 0.
- Second definition as "stable" if the difference in the MMSE score between baseline and 1-year follow-up was ≥ -1. Definition as "decliner" if that difference was < -1.
- Third definition as "stable" if the difference in the MMSE score between baseline and 1-year follow-up was ≥ +1. Definition as "decliner" if that difference was < +1.

The results of the ML experiments with those three definitions were averaged to obtain prediction accuracy (%) less affected by measure errors of one point in the MMSE score.

To test the prediction performance of each AI tool (i.e., SLO, LOG, 3-NN, and SVM), we used the five-fold cross-validation strategy with twenty runs to reduce the bias introduced by the random shuffling of individual datasets used in the training group (70% of the datasets) and the testing group (30%). The results reported in this article were computed by averaging those obtained by the twenty runs performed.

The following percentage indexes represented the performance of the above AI tools in the prediction: (1) sensitivity to measure the rate of "decliners" correctly classified; (2) specificity to measure the rate of the "stable" correctly classified; and (3) accuracy as the mean between the sensitivity and specificity weighted for the number of "decliners" and "stables.".

The performance of the AI tools in prediction was assessed using the following metrics: (1) sensitivity, which measures the rate of correctly

classified "decliners"; (2) specificity, which measures the rate of correctly classified "stable" individuals; and (3) accuracy, calculated as the weighted mean of sensitivity and specificity, accounting for the proportion of "decliners" and "stables" in the dataset.

Additionally, we evaluated the classification accuracy using several other metrics, including the mean of the Kappa statistic, the F-measure, and the Area Under the Receiver Operating Characteristic Curve (AUROCC). Cohen's Kappa statistics (Landis and Koch, 1977) compare the observed accuracy with the expected accuracy under random chance, providing a measure of agreement beyond chance. The F-score (van Rijsbergen, 1979) is used to evaluate the accuracy of a binary classification model, combining precision and recall into a single metric. Lastly, the AUROCC is a performance measure for classification problems across various threshold settings. The ROC curve represents the trade-off between true positive and false positive rates, and the AUC indicates the model's ability to distinguish between classes (Zou et al., 2007).

Notably, we conducted a preliminary study on the study database to select the optimal hyperparameters for the ML tools used to predict disease course in ADMCI patients. The findings from this preliminary study were presented at the 21st International Conference on "Image Analysis and Processing—ICIAP 2022″ (Lecce, Italy, May 23–27, 2022) and published in the corresponding Conference Proceedings (Fontanella et al., 2022). We utilized "accuracy" as the evaluation metric for predicting cognitive decline ("stable" vs. "decliner") in ADMCI patients. The dataset was divided into a training set (70%) and a validation set (30%). A grid of hyperparameters was established for each ML tool. Specifically, we defined the maximum depth of trees and minimum samples per leaf for the Simple Logistic Regression Model Trees, "L" regularization parameters for Logistic Regression, the number of neighbors and distance metrics for the K-Nearest Neighbor, and the kernel type, regularization parameter, and kernel-specific parameters for the Support Vector Machine. Subsequently, the best hyperparameter set was selected based on accuracy, and its generalizability was evaluated by evaluating the ML model on a separate validation set. To control overfitting, we monitored the difference between training and validation scores.

2.11. Stratification of ADMCI patients according to age

Considering the substantial clinical differences in the onset and progression of clinical manifestations in AD as a function of patients' age (Licht et al., 2007; Seath et al., 2023; Wattmo et al., 2017; Babiloni et al., 2021b), the AI tools were separately evaluated in the following two ADMCI groups.

The youngest ADMCI group of persons with < 70 years old ($N = 31$, 11 males) had a percentage of *APOE4* carriers of 80%, an age range and mean of 56–69 and 64.4 ± 0.2 years SE, education attainment years of 11.7 ± 0.6 SE, a baseline MMSE score of 26.2 ± 0.2 SD, and $N = 17$ "decliners" (55%).

The oldest ADMCI group of persons ≥ 70 years old ($N = 32$, 13 males) had a percentage of *APOE4* carriers of 66%, an age range and mean of 70–81 and 73.9 ± 0.4 years SE, education attainment years of 10.9 ± 0.5 SE, a baseline MMSE score of 26.4 ± 0.2 SE, and $N = 16$ "decliners" (55%).

The above arbitrary stratification allowed us to evaluate the main study hypothesis with two groups of ADMCI patients matched as mean age, mean education attainment, *APOE* genotyping, and gender (statistical non-parametric tests showing differences with $p > 0.05$ uncorrected). Furthermore, the two ADMCI groups were also matched in global cognitive status as revealed by the MMSE score (statistical non-parametric tests showing differences with $p > 0.05$ uncorrected).

In ADMCI patients, the use of selective serotonin reuptake inhibitors (SSRIs), selective serotonin and noradrenaline reuptake inhibitors (SNRIs), benzodiazepines (BZDs), non-benzodiazepines GABA acting agent (No BZDs), acetylcholinesterase inhibitors (AChEIs), and N-methyl-D-aspartate receptors (NMDARs) were controlled. The ADMCI patients using those drugs could take their medications immediately after rsEEG experiments, planned in the late morning. Therefore, they just delayed the assumption of their medications for a few hours more than their normal routine. No statistically significant difference was found between the youngest and oldest ADMCI groups using the above medications, even when a threshold of $p < 0.05$ uncorrected was used.

3. Results

3.1. Characterization of the ADMCI patients based on the neuropsychological test scores

Table 3 reports the mean score values (± SE) of the following neuropsychological tests administered in the ADMCI patients to characterize them towards the future cross-validation of the present results: ADAS-Cog, Rey Auditory Verbal Learning Test (immediate and delayed recall), Trail Making Test (B-A), Verbal fluency for letters, Verbal fluency for the category, and Clock (drawing and copy). Furthermore, Table 3 includes the cut-off (threshold) scores defining the percentage of ADMCI patients with abnormal values in those tests according to standard normative thresholds.

3.2. Characterization of the ADMCI patients based on the structural MRI markers

Table 4 reports the mean score values (± SE) of the following T1-weighted MRI markers in the ADMCI patients to characterize them towards the future cross-validation of the present results: (1) global markers (white matter and gray matter volumes normalized for the total intracranial volume; total cortical thickness); (2) ventricular markers (lateral ventricle volume normalized for the total intracranial volume); (3) vascular lesion markers (subcortical white matter hypointensity); (4) mesial temporal lobe markers (hippocampus and amygdala volumes normalized for the total intracranial volume; entorhinal thickness); and (5) basal ganglia markers (caudate nucleus, putamen nucleus, pallidum nucleus, and accumbens nucleus normalized for the total intracranial volume).

3.3. Characterization of the ADMCI patients based on the neurophysiological (rsEEG) markers

In the Nolder group, the eLORETA solutions showed maximum magnitude in the rsEEG occipital (maximum), parietal, and temporal alpha 2 and alpha 3 sources. Compared to the Nolder group, the ADMCI group showed a substantial decrease in the eLORETA solutions in

Table 3
Mean score values (± SE) derived from the neuropsychological tests and the percentage (%) of ADMCI patients with abnormal values for those tests. The table also reports the test cut-off (threshold) scores, which define the abnormality of the ADMCI patient's performance according to standard normative data. Legend: RAVTL: Rey Auditory Verbal Learning test.

Neuropsychological test scores in the ADMCI patients		
	Cut-off of abnormality	**Mean ± SE *(% subjects with abnormal score)***
ADAS-Cog	*≥ 17*	20.4 ± 1.2 (72.7%)
Trail Making Test B-A	*≥ 187*	128.6 ± 12.0 (25.0%)
RAVLT immediate recall	*< 28.53*	30.2 ± 1.8 (44.1%)
RAVLT delayed recall	*< 4.69*	3.6 ± 0.5 (73.5%)
Clock drawing	*> 3*	3.8 ± 0.2 (76.5%)
Clock copy	*> 3*	4.5 ± 0.2 (85.3%)
Letter fluency	*< 17*	34.2 ± 2.1 (8.8%)
Letter category	*< 25*	33.3 ± 2.2 (29.4%)

Table 4
Mean score values (± SE) of the structural magnetic resonance imaging (sMRI) markers derived from the ADMCI patients of the present study. Regional markers were selected as more intricately linked to AD neurodegeneration. Legend: WM: total brain white matter; GM: total brain gray matter.

Structural magnetic resonance imaging (sMRI) markers in the ADMCI patients	
Global markers	
Normalized WM volume	0.275 ± 0.003
Normalized GM volume	0.391 ± 0.005
Cortical thickness	4.72 ± 0.05
Basal Ganglia markers	
Normalized caudate volume	0.0046 ± 0.0001
Normalized putamen volume	0.0058 ± 0.0001
Normalized pallidum volume	0.0025 ± 0.0001
Normalized accumbens volume	0.00057 ± 0.00002
Mesial Temporal markers	
Normalized hippocampus volume	0.0048 ± 0.0001
Normalized amygdala volume	0.0019 ± 0.0001
Entorhinal cortical thickness	6.53 ± 0.12
Ventricular markers	
Normalized lateral ventricle volume	0.021 ± 0.001
Hypointensity/lesion WM markers	
WM hypointensity	2,580 ± 291
WM lesions	2,789 ± 600

posterior (i.e., parietal, occipital, and temporal) rsEEG alpha 2 and alpha 3 sources. Furthermore, the ADMCI group showed a substantial increase in the eLORETA solutions in widespread rsEEG delta sources.

The ANOVA results of the regional rsEEG source activations (i.e., normalized eLORETA solutions) showed a statistically significant interaction effect ($F = 15.3$; $p < 0.0001$) among the factors Group (Nolder and ADMCI), Band (delta, theta, alpha 1, alpha 2, alpha 3), and ROI (frontal, central, parietal, occipital, temporal, and limbic).

The Duncan planned post-hoc testing with a statistical threshold of $p < 0.0001$ showed what follows: (1) the discriminant pattern Nolder > ADMCI was fitted by central, parietal, occipital, temporal, and limbic rsEEG alpha 2 source activities as well as central, parietal, occipital, temporal, and limbic rsEEG alpha 3 source activations; (2) the discriminant pattern Nolder < ADMCI was fitted by the frontal, central, parietal, and temporal rsEEG delta source activations.

Notably, these findings were not due to outliers from those individual eLORETA solutions (log-10 transformed), as shown by Grubbs' test with an arbitrary threshold of $p > 0.001$ (Fig. 2).

3.4. *Performances of the AI tools in the prediction of the cognitive decline in ADMCI patients*

Table 5 reports the original results of the present study on the prediction of the cognitive status of "decliners" or "stable" in the ADMCI patients evaluated at the 1-year follow-up, based on four independent AI tools of machine learning (i.e., SLO, LOG, 3-NN, and SVM) using standard biomarkers of rsEEG, sMRI, CSF, and all those modalities together for the training and testing phases of the procedure. As mentioned above, the rsEEG, sMRI, and CSF biomarkers were enriched with basic information typically available on the first visit of an AD patient in a memory clinic: sex, age, education attainment, and *APOE* genotyping. ADMCI patients were stratified into one group with individuals having < 70 years and another with individuals having ≥ 70 years. Performances among the four classifiers and the three thresholds were averaged.

In the patients of the youngest ADMCI group (< 70 years), the prediction of the cognitive status of "decliners" or "stable" showed a moderate accuracy with the above biomarkers: (1) sensitivity of 61.6% for the "decliners" and specificity of 71.3% for the "stable" patients from the enriched rsEEG biomarkers; (2) sensitivity of 70% for the "decliners" and specificity of 72.5% for the "stable" patients from the enriched sMRI biomarkers; (3) sensitivity of 50.9% for the "decliners" and specificity of 75.1% for the "stable" patients from the enriched CSF biomarkers; and (4) sensitivity of 75.3% for the "decliners" and specificity of 73.2% for the "stable" patients from the all those biomarkers used together as a

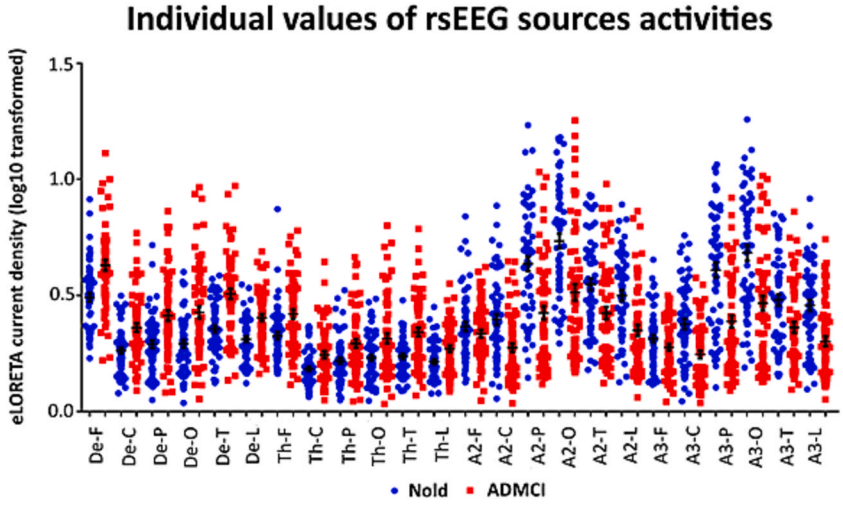

Fig. 2. Individual and group mean values of the normalized regional cortical source activations estimated from rsEEG source activations estimated in ADMCI patients and Nolder participants used as controls. Those cortical rsEEG source activations were estimated using eLORETA (https://www.uzh.ch/keyinst/loreta.htm). The rsEEG sources estimation was performed for individual delta, theta, alpha 1, alpha 2, and alpha 3 frequency bands in the following lobar cortical regions of interest of the eLORETA source space: frontal, central, parietal, occipital, temporal, and limbic. For each individual, the normalization of the eLORETA source solution for a given frequency bin was performed based on the ratio with the mean of all eLORETA source solutions estimated at all sources of the cortical model from 0 to 45 Hz. In the figure, each dot represents the normalized log-10 transformed eLORETA source solution for a given frequency band and cortical region of interest. For each frequency band and cortical region of interest, the group mean value of the eLORETA source solution is indicated by a horizontal segment. In contrast, the vertical segment represents the standard error of the mean. Abbreviations: De-F = frontal delta; De-C = central delta; De-P = parietal delta; De-O = occipital delta; De-T = temporal delta; De-L = limbic delta; Th-F = frontal theta; Th-C = central theta; Th-P = parietal theta; Th-O = occipital theta; Th-T = temporal theta; Th-L = limbic theta; A2-F = frontal alpha 2; A2-C = central alpha 2; A2-P = parietal alpha 2; A2-O = occipital alpha2; A2-T = temporal alpha2; A2-L = limbic alpha2; A3-F = frontal alpha 3; A3-C = central alpha 3; A3-P = parietal alpha 3; A3-O = occipital alpha3; A3-T = temporal alpha3; and A3-L = limbic alpha3. *Legend: rsEEG = resting-state eyes-closed electroencephalographic; ADMCI = Alzheimer's disease at the prodromal stage of amnesic mild cognitive impairment; Nolder = cognitively unimpaired normal old seniors.*

Table 5
Performance (%) of the machine learning (ML) tools used for the prediction of the cognitive status of "decliners" or "stable" ADMCI patients evaluated at the 1-year follow-up. Each ADMCI individual was classified as "stable" or "decliner" based on the difference in the MMSE score between the baseline and 1-year follow-up (for details, see the section "Methods"). Specifically, the results concern the averaged performances of the four ML tools among three different thresholds to define each ADMCI individual as "stable" according to the difference in the MMSE score baseline minus 1-year follow-up: (i) $\geq$ -1, (ii) $\geq$ 0, and (iii) $\geq$ +1. The results of the ML experiments with those three definitions were averaged to obtain prediction accuracy (%) less affected by measure errors of one point in the MMSE score. The following AI tools were used: Simple Logistic Regression Model Trees (SLO), Logistic Regression (LOG), K-Nearest Neighbor (K-NN), and Support Vector Machine (SVM). For each tool, the prediction was based on standard resting-state eyes-closed electroencephalographic (rsEEG) data, structural magnetic resonance imaging (sMRI) data, and cerebrospinal fluid (CSF) biomarkers, enriched with information derived from APOE4 genetic risk of AD, age, sex, and education attainment data. The performance of the AI tools was indexed with the following percentage indexes: (1) sensitivity to measure the rate of "decliners" correctly classified; (2) specificity to measure the rate of the "stable" patients correctly classified; and (3) accuracy as the mean between the sensitivity and specificity weighted for the number of "decliners" and "stable" patients. The ADMCI patients were stratified into one group with individuals having $<$ 70 years and another group with individuals having $\geq$ 70 years.

Machine learning tools (SVM, 3-NN, LOG, and SLO) performances			
ADMCI Age $\geq$ 70 years			
Accuracy (%)	**Sensitivity (%)**	**Specificity (%)**	**Markers**
76.6	60.4	76.5	rsEEG
78.2	65.5	79.3	sMRI
77.7	67.8	74.8	CSF
77.3	68.6	71.2	ALL together
ADMCI Age < 70 years			
Accuracy (%)	**Sensitivity (%)**	**Specificity (%)**	**Markers**
73.8	55.7	72.3	rsEEG
76.6	62.0	69.0	sMRI
71.3	52.7	63.9	CSF
76.2	63.0	64.6	ALL together

gold standard.

In the patients of the oldest ADMCI group $\geq$ 70 years, the AI tool predicted the patients' cognitive status a bit better: (1) sensitivity of 73% for the "decliners" and specificity of 80.1% for the "stable" patients from the enriched rsEEG biomarkers; (2) sensitivity of 66.9% for the "decliners" and specificity of 76.9% for the "stable" patients from the enriched sMRI biomarkers; (3) sensitivity of 77.3% for the "decliners" and specificity of 66.2% for the "stable" patients from the enriched CSF biomarkers; and (4) sensitivity of 77% for the "decliners" and specificity of 78.1% for the "stable" patients from the all those biomarkers used together.

Table 6 provides additional information on prediction accuracy. Specifically, it reports on Kappa statistics, F-measure, and ROC area for the average performances among the four classifiers and the three thresholds. Furthermore, for the sake of completeness, Supplementary Material Tables 1-12 (SM1-SM12) in the Supplementary Materials report the prediction accuracy for each definition of cognitive decline (see "Methods") and each machine learning tool used.

3.5. Control analysis on the association among rsEEG, enrichment variables, and global cognition

As mentioned above, APOE genotyping, age, sex, and educational attainment are expected to interact in a complex manner with cognitive decline in ADMCI patients and AD-related neuropathological, neurophysiological, and neurodegenerative processes, as reflected by CSF Abeta/p-tau, rsEEG rhythms, and sMRI variables, respectively. Considering our primary interest in the present global rsEEG measures, we investigated the weight of the linear relationship between these

Table 6
Performance (%) of the ML tools used for the prediction of the cognitive status of "decliners" or "stable" ADMCI patients evaluated at the 1-year follow-up. Each ADMCI individual was classified as "stable" or "decliner" based on the difference in the MMSE score between the baseline and 1-year follow-up (for details, see the section "Methods"). Specifically, the results concern the averaged performances of the four ML tools among three different thresholds to define each ADMCI individual as "stable" according to the difference in the MMSE score baseline minus 1-year follow-up: (i) $\geq$ -1, (ii) $\geq$ 0, and (iii) $\geq$ -1. The results of the ML experiments with those three definitions were averaged to obtain prediction accuracy (%) less affected by measure errors of one point in the MMSE score. For each tool, the prediction was based on standard resting-state eyes-closed electroencephalographic (rsEEG) data, structural magnetic resonance imaging (sMRI) data, and cerebrospinal fluid (CSF) biomarkers, enriched with information derived from APOE4 genetic risk of AD, age, sex, and education attainment data. The performance of the AI tools was indexed with the following percentage indexes: (1) Kappa statistics, (2) F-measure, and (3) Area Under the Receiver Operating Classifier Curve (AUROCC). The ADMCI patients were stratified into one group with individuals having $<$ 70 years and another group with individuals having $\geq$ 70 years.

Artificial intelligence tool (SVM, 3-NN, LOG, and SLO) performances			
ADMCI Age $\geq$ 70 years			
KAPPA	**F-MEASURE**	**AUROCC**	**Markers**
0.47	0.79	0.68	rsEEG
0.40	0.68	0.70	sMRI
0.42	0.75	0.68	CSF
0.49	0.78	0.76	ALL together
ADMCI Age < 70 years			
KAPPA	**F-MEASURE**	**AUROCC**	**Markers**
0.27	0.65	0.56	rsEEG
0.23	0.63	0.60	sMRI
0.36	0.71	0.69	CSF
0.33	0.70	0.68	ALL together

measures and APOE genotyping, age, sex, and educational attainment in explaining cognitive decline at 1-year follow-up in all ADMCI participants as a whole group. To this aim, we performed an explorative control regression analysis using both general linear regression and binomial regression models ($p < 0.05$). The results are reported in detail in the Supplementary Material (Results). Briefly, a significant association was found only between the global rsEEG alpha 2, beta 1, and beta 2 source activities and sex ($p < 0.05$). This finding suggests that the association between the global rsEEG measures and the above variables may not be linear, supporting the use of ML tools to tackle it in ADMCI patients.

4. Discussion

In the present retrospective study, a new methodological approach of machine learning was used to predict the cognitive status, "stable" vs. "decliner," in ADMCI patients evaluated at 1-year follow-ups, based on regional rsEEG source activity estimated from enriched rsEEG biomarkers from delta to alpha frequency bands, the enrichment is based on sex, age, education attainment, and *APOE* genotyping. These biomarkers reflect the brain neurophysiological (pathophysiological) mechanisms that regulate the global cortical excitability (arousal) and the vigilance/consciousness levels in quiet wakefulness (Babiloni et al., 2021b). This approach combined four independent, standard machine learning tools to mitigate their possible computational biases (i.e., Simple Logistic regression Model Trees, Logistic regression, K-Nearest Neighbor, and Support Vector Machine; see the "Methods" for more details). Along this line, their predicting performances were averaged to index the prediction accuracy.

In this exercise, the prediction accuracy of the enriched rsEEG biomarkers was compared with that obtained using enriched CSF biomarkers of AD neuropathology (i.e., brain amyloidosis and tauopathy) and sMRI biomarkers of brain neurodegeneration (i.e., cortical

thickness, brain, and hippocampus gray matter volume) of the so-called A-T-N(C) Framework for the AD diagnosis in clinical research studies (Jack et al., 2018). Finally, the clinically relevant "age factor," underlying differences in clinical presentation and course of AD (Licht et al., 2007; Seath et al., 2023; Wattmo et al., 2017; Babiloni et al., 2021b), was considered by stratifying the ADMCI patients into two groups substantially matched as numerosity, gender, and education attainment: the group of ADMCI patients having < 70 years and that of ADMCI patients having ≥ 70 years.

The combined machine learning tools demonstrated the highest prediction accuracy in the oldest ADMCI patients (≥ 70 years), with accuracy rates of 76.6% using enriched rsEEG biomarkers, 78.2% using enriched sMRI biomarkers, 77.7% using enriched CSF biomarkers, and 77.7% when all enriched rsEEG, sMRI, and CSF biomarkers were considered together. In the youngest ADMCI patients (< 70 years), the prediction accuracy was 73.8% with enriched rsEEG biomarkers, 76.6% with enriched sMRI biomarkers, 71.3% with enriched CSF biomarkers, and 76.2% when all enriched rsEEG, sMRI, and CSF biomarkers were used together.

The present results complement and extend those of previous studies showing that the spectral rsEEG biomarkers from delta to alpha frequency bands were able to predict cognitive decline in groups of patients with ADSCD and ADMCI at about 1-year follow-ups or even later (Prichep et al., 1994, 2006, 2014; Nobili et al., 1999; Jelic et al., 2000; Huang et al., 2000; Rossini et al., 2006; Luckhaus et al., 2008; Babiloni et al., 2014; Gouw et al., 2017). As a novelty from those studies, the present investigation enriched the spectral rsEEG measures with information derived from *APOE* status (Babiloni et al., 2006), age (Babiloni et al., 2021b), sex (Babiloni et al., 2022), and education attainment (Babiloni et al., 2021c). Furthermore, it combined independent AI tools to specify the prediction accuracy (sensitivity and specificity) of the cognitive decline at the individual level. The results enlightened a global picture and the potential for using the present approach with enriched rsEEG biomarkers and combined AI tools in a real-world clinical context.

The present results build upon and expand the findings of several previous investigations that utilized rsEEG markers as inputs for machine learning tools in the classification and prediction of ADMCI and ADD patients. A summary of the key findings from these prior studies is provided in Table SM13 (Supplementary Materials). Comparing our results with those of previous studies, the following observations can be made:

Approximately 50% of the reviewed studies involved a smaller cohort of ADMCI and ADD patients compared to our study.

Only eight machine learning studies specifically aimed to predict the clinical status of AD at follow-ups, which aligns with the objective of the present study. The reported accuracy in these predictive studies ranged from 61% to 90%, with an average accuracy of 79%.

Most of the reviewed studies focused on classifying older adults (Nolder) versus AD participants based on rsEEG markers, with most achieving a classification accuracy of over 85%.

Unlike previous studies, the present study uniquely compares prediction accuracy at follow-ups across rsEEG, sMRI, and CSF diagnostic biomarkers.

Additionally, our study is distinct in averaging the prediction accuracy across four traditional machine learning tools rather than reporting only the best-performing model. While this methodological approach slightly reduced the clinical prediction accuracy for ADMCI patients to 77%, it ensures that the findings are robust and generalizable, offering valuable insights for potential prognostic clinical applications.

In contrast, most previous machine learning investigations focused on classifying Nolder versus AD participants based on rsEEG markers, typically achieving a classification accuracy of over 85%.

4.1. The age factor in predicting cognitive decline in ADMCI patients

In the present study, the enriched rsEEG and CSF biomarkers showed worse performances in the youngest ADMCI patients having < 70 years, suggesting a complex interaction of age with the AD-related neuropathology, neurophysiological oscillatory mechanisms generating rsEEG rhythms and regulating cortical arousal, and other constitutional and environmental factors (Marshall and Cooper, 2017; Meyers et al., 2021; Babiloni et al., 2021a). More specifically, it can be speculated that AD patients' age may interact with the following factors: (1) the *APOE* genetic risk related to the early accumulation of AD neuropathology probed by the CSF Aβ1-42 and phospho tau levels; (2) the vulnerability of the female brains to AD neuropathology; (3) the impact of AD neuropathology on brain neurophysiological oscillatory mechanisms regulating the cortical arousal revealed by rsEEG abnormalities; (4) the brain neurodegeneration unveiled by sMRI markers; and (5) the neuroprotective/compensatory role against the AD neuropathology of the "cognitive reserve" estimated using the education attainment.

The above interaction may result in the distinct features observed in early- (EOAD) and late-onset (LOAD) AD patients (Rossor et al., 2010). Previous studies showed that EOAD was often typified by the frontal executive, language, and visuospatial dysfunctions associated with structural and functional impairments in frontal and parietal cortical regions, whereas LOAD was frequently characterized by an early amnesic syndrome related to structural and functional impairments in the medial temporal lobe and limbic regions (Frisoni et al., 2007; Möller et al., 2013; van der Flier et al., 2014; Ossenkoppele et al., 2015; Pini et al., 2020). These effects were coupled with greater tauopathy (1) in the parieto-occipital cortex and visuo-spatial deficits in EOAD patients and (2) in temporal areas and memory deficits in LOAD patients (Cho et al., 2017). Compared to the LOAD patients, EOAD patients also showed more abnormal rsEEG delta/theta and alpha rhythms (de Waal et al., 2012; Babiloni et al., 2021b; Özbek et al., 2021), with paradoxically less intense alterations of rsEEG rhythms in *APOE4* carriers (de Waal et al., 2011).

Considering the above data, it can be speculated that the heterogeneity of the pathological processes and the complexity of their interaction may cause the relatively low predicting performances of the enriched rsEEG and CSF biomarkers in ADMCI patients having < 70 years. They may also explain the mixed literature findings on the cognitive decline rate in EOAD and LOAD patients. Some previous studies showed no differences in the cognitive decline rate between EOAD and LOAD groups (Grønning et al., 2012; Almkvist and Nordberg, 2023). In other studies, compared to LOAD patients, EOAD patients showed a faster decline at 1-year follow-up (van der Vlies et al., 2009) or $\geq$ 2-year follow-ups (Jacobs et al., 1994; Wilson et al., 2000; Wattmo and Wallin, 2017) regardless of the symptom duration, sex, and baseline cognitive performance. Furthermore, the EOAD patients showed more abnormal CSF biomarkers of AD, regardless of age, disease duration, and education attainment (Koric et al., 2010; Wallin et al., 2010). Notably, education attainment might partially counteract the AD-related neuropathological and neurophysiological oscillatory processes generating rsEEG rhythms in EOAD patients (Stern et al., 2018; Babiloni et al., 2021b) but could not make predictable the progression of cognitive deficits as in LOAD patients. In this speculative line, compared to LOAD patients, EOAD patients may have cognitive decline more dependent on the effects of brain neuroinflammation, neuroimmune reactivity, and vascular dysfunctions, not probed by proper biomarkers in the present study. Therefore, a better prediction of the cognitive decline in ADMCI patients having ≥ 70 years may require the inclusion of additional CSF or blood plasma biomarkers reflecting the following pathological processes: (1) neuronal injury (e.g., serum visinin-like protein-1 and neurofilament light); (2) neuroinflammation (e.g., triggering receptor expressed on myeloid cells 2; YKL-40, a member of mammalian chitinase-like proteins; osteopontin; autoimmune glial fibrillary acidic protein astrocytopathy, GFAP; progranulin; and monocyte chemoattractant protein-1, MCP-1); (3) synaptic dysfunction (synaptosomal-associated protein 25, SNAP-25, and axon growth and neuroplasticity, GAP-43); (4) vascular dysregulation (heart-type fatty acid binding

protein, hFABP); and (5) co-occurrent neuropathology (α-synuclein levels and TDP-43 pathology). Indeed, the above pathological processes and biomarkers are attracting increasing interest in constructing a modern model of AD (McGrowder et al., 2021).

4.2. Methodological Considerations

This retrospective and exploratory study utilized clinical and rsEEG datasets, primarily from the PDWAVES Consortium archive (https://www.pdwaves.eu). The interpretation of the present findings must consider several methodological limitations. These include (i) the relatively small sample size of AD patients (N = 63), partially justified by a well-characterized diagnosis of ADMCI based on extensive clinical and neuropsychological assessments and confirmed by positive diagnostic CSF biomarkers for Aβ1-42 and phospho-tau; (ii) the availability of data from only a single follow-up session occurring one year after baseline, as per standard clinical practice; (iii) the reliance on rsEEG input features derived solely from eLORETA-based rsEEG source solutions estimated within broad cortical regions of interest, due to the relatively low resolution of rsEEG recordings (e.g., 19 scalp electrodes) used in this clinical context; (iv) the use of only four traditional, independent ML tools, with no application of explainable artificial intelligence (XAI) methods; and (v) the use of only the "traditional" MMSE score to characterize patients' cognitive decline over time, partially justified by the fact that all ADMCI patients received the confirmation of their MCI status at that the follow-up by clinical and MRI exams.

Regarding the above methodological limitations, it is worth noting that the Mini-Cog test, Addenbrooke's Cognitive Examination-Revised, and Montreal Cognitive Assessment demonstrate comparable or even superior diagnostic performance compared to the MMSE (Tsoi et al., 2015). However, we opted for the use of the MMSE score and eLORETA source estimation because they are "universal" and have a significant background of successful previous clinical applications in patients with ADMCI. Furthermore, MMSE is translated and calibrated in practically any language, which is an important characteristic considering that the present study includes European and Asian clinical centers.

Along the same line, eLORETA cannot be considered the best procedure for estimating cortical sources of rsEEG rhythms to probe the neurophysiological oscillatory mechanisms underlying the regulation of vigilance in quiet wakefulness and to enrich disease models for the prodromal AD stages. However, eLORETA is a freeware program with a comprehensive manual available in English. We have repeatedly used it in our previous rsEEG studies in ADMCI patients as a reference for this study (Babiloni et al., 2021b, Babiloni et al., 2021c; 2022). Furthermore, we aimed for any clinical center to be able to implement the current clinical and instrumental procedures to replicate these study findings and enhance the local clinical assessment of ADMCI patients.

Given these limitations, the results of the present study require cross-validation and extension in future research using improved methodologies.

Specifically, future studies should utilize new techniques for assessing cognitive status in ADMCI patients, such as exergaming, a combination of exercise and gaming (Chan et al., 2024). Indeed, virtual reality-based exergaming has been drawing the attention of individuals with MCI and demonstrating effectiveness in enhancing cognitive function when used as brain training techniques (Chan et al., 2024). This technique could also be used for early disease screening. As a quite simple way of exergaming to be used as a screening test for cognitive decline, finger tapping measurements have also gained attention, as dexterity in hand movements can reveal signs of dementia (Kluger et al., 1997; Sano et al., 2025).

In future studies, advanced EEG techniques may enhance the EEG biomarkers used as input for predicting cognitive decline in ADMCI patients. These techniques may use more than 48 scalp electrodes and source connectivity estimators, along with advanced rsEEG feature extraction methods (Marino et al., 2016; Liu et al., 2018). Advanced EEG feature extraction methods for future research could include stationary wavelet entropy and predator–prey particle swarm optimization, discrete wavelet transform, empirical mode decomposition, and single-slice-based detection for Alzheimer's disease via wavelet entropy and a multilayer perceptron trained by biogeography-based optimization (Wang et al., 2018; Subasi, 2020).

Finally, the incorporation of ML and deep learning approaches, such as artificial neural networks, random forest, bagging, XGBoost, (bidirectional) long short-term memory, convolutional neural networks, and deep belief network architectures, would enhance the present analysis (Jung et al., 2021; Liang et al., 2021; Arya et al., 2023). It is worth noting that while deep learning methods reduce the need for extensive human intervention, they would require a much larger dataset than the one used in this study and could pose challenges related to the interpretability and explainability of the results (Arya et al., 2023). Transparent XAI tools that provide explanations for their predictions facilitate fair, unbiased, reliable, and reasonable AI based on medical characteristics, rather than spurious correlations, by allowing users to understand better the factors that contributed to a prediction (Allgaier et al., 2023).

5. Conclusions

This exploratory study evaluated the accuracy of combined AI-ML tools in predicting the cognitive decline in ADMCI patients at 1-year follow-ups based on enriched rsEEG biomarkers (lobar rsEEG source activities from delta to alpha bands). The MMSE score measured this decline. It is widely used in memory clinics as a measure of global cognitive status. In the experimental design, enriched CSF (Abeta/p-tau) and sMRI (white and gray matter volume measures, etc.) biomarkers of the A-T-N(C) Framework served as a reference (Jack et al., 2018). All biomarkers were enriched by APOE genotyping, sex, age, and education attainment information typically available on the first visit to memory clinics. The target of the prediction was the patient's cognitive status at 1-year follow-ups ("stable" vs. "decliner").

The combined AI tools showed the most accurate predictions in the oldest ADMCI patients ($\geq$ 70 years): 76.6% from the enriched rsEEG biomarkers, 78.2% from the enriched sMRI biomarkers, 77.7% from the enriched CSF biomarkers, and 77.7% using all the enriched rsEEG, sMRI, and CSF biomarkers considered together. In the youngest ADMCI patients ($<$ 70 years), the prediction showed 73.8% from the enriched rsEEG biomarkers, 76.6% from the enriched sMRI biomarkers, 71.3% from the enriched CSF biomarkers, and 76.2% using all the enriched rsEEG, sMRI, and CSF biomarkers considered together.

Our results showed moderate prediction accuracy of cognitive decline in ADMCI patients aged $\geq$ 70 years using standard ML tools implemented in many software platforms (e.g., MATLAB, Python, etc.) and noninvasive and cost-effective rsEEG biomarkers enriched with the above demographic and disease risk variables. These rsEEG biomarkers provided predicting values like those of the CSF and sMRI biomarkers enriched with the same variables. This outcome underscores the potential of rsEEG biomarkers in the instrumental assessment of ADMCI patients. Overall, the present results motivate future cross-validation longitudinal studies using larger samples of ADMCI patients, more disease risk/protective facts (e.g., lifestyle, physical activity, socioeconomic, socio-affective, and environmental factors), and serial follow-ups to address the statistical comparison of the AI-tool predictive performances between the enriched rsEEG, sMRI, and CSF biomarkers.

The findings suggest that the combined AI tools offer moderate prediction accuracy for cognitive decline in ADMCI patients aged 70 years and older. This is achieved using standard, non-invasive, and cost-effective rsEEG biomarkers. Notably, the predictive performance of these biomarkers was comparable to that of CSF and sMRI biomarkers.

These rsEEG biomarkers may probe the neurophysiological oscillatory mechanisms underlying the generation of rsEEG rhythms and the regulation of cortical arousal and vigilance during quiet wakefulness (Babiloni, 2022; Babiloni et al., 2021a). This brain function is highly

relevant to the quality of life of AD patients, as it supports the ability to maintain sufficient vigilance to watch gentle or non-demanding television programs (e.g., simple in narrative and calming, such as nature documentaries, light entertainment shows, etc.) and engage in social conversations with friends and relatives.

Declaration of competing interest

The authors declare that they have no known competing financial interests or personal relationships that could have appeared to influence the work reported in this paper.

Acknowledgments

The present study was developed based on the data of the PDWAVES Consortium (www.pdwaves.eu) and the PharmaCog project (https://www.imi.europa.eu/projects-results/project-factsheets/pharma-cog). The Partners and institutional affiliations are reported on the cover page of this manuscript.

In this study, the clinical, cerebrospinal fluid, neuropsychological, and magnetic resonance imaging data analyses were partially supported by the funds of "Ricerca Corrente 2022-2023" attributed by the Italian Ministry of Health to the IRCCS Synlab SDN of Naples (Italy), IRCCS Ospedale San Martino of Genoa (Italy), Oasi Research Institute-IRCCS, Troina (Italy), the IRCCS Fatebenefratelli of Brescia, and IRCCS San Raffaele Pisana of Rome (Italy).

Prof. Claudio Babiloni was partially supported by the funds of the project titled "Rome Technopole" from the Call "Piano Nazionale di Ripresa e Resilienza (PNRR)- Mission 4 "Istruzione e Ricerca" - Component 2 – "Investment 1.5," granted by European Union - Next Generation EU, Italian Ministry of University and Research;" Grant Agreement: ECS00000024 and was also partially supported by a HORIZON 2021 project grant titled "eBRAIN-Health – Actionable Multilevel Health Data", Call and Sponsor: HORIZON 2021, HORIZON-INFRA-2021-TECH-01 (HORIZON-INFRA-2021-TECH-01-01 – Interdisciplinary digital twins for modeling and simulating complex phenomena at the service of research infrastructure communities), Grant Agreement: GAP-101058516.

Prof. Matteo Pardini and Claudio Babiloni were partially supported by the funds of the project titled "SleepAD—Integrated Multi-parametric Imaging, Neurophysiological Biomarkers, and Artificial Intelligence to Study the Relationships Among Sleep Disorders, Glymphatic System Dysfunctions, Brain Amyloidosis and Connectivity, and Epileptiform Activity in Prodromal Alzheimer's Disease" (Call and Sponsor: PE00000006 "PNRR MUR-M4C2-MNESYS–A multiscale integrated approach to the study of the nervous system in health and disease (MNESYS)"—EXTENDED PARTNERSHIP #12, SPOKE 6, and CASCADE CALL from PNRR, Mission 4, Component 2, Investment, CUP: D33C22001340002).

Prof. Claudio Del Percio was partially supported by the funds of the project titled "Amyloid-related cortical excitability in patients with MCI due to Alzheimer's disease" from the Call "ANNUAL STRATEGIC PROGRAM OF ITALIAN MINISTRY OF UNIVERSITY AND SCIENTIFIC AND TECHNOLOGICAL RESEARCH" Grant Agreement: 2022FJAXY8, CUP B53D23018610006).

Prof. Fabrizio Stocchi was partially supported by the funds of the project titled "Effects of endogenous and exogenous risk factors in patients with Alzheimer's and Parkinson's diseases using clinical indexes and endophenotypes (biomarkers) as inputs to artificial intelligence (PREDICT-NEURODEGEN)" from the Call "ANNUAL STRATEGIC PROGRAM OF ITALIAN MINISTRY OF HEALTH;" Grant Agreement: PNRR-MAD-2022-12376415.

Prof. Raffaele Ferri was partially supported by the funds of the project titled "Integrating sleep-wake oscillatory activities and liquid biopsy as innovative biomarkers for multimodal diagnosis in preclinical and prodromal Alzheimer's disease (ISLA)" from the Call "ANNUAL STRATEGIC PROGRAM OF ITALIAN MINISTRY OF HEALTH;" Grant Agreement: PNRR-MCNT2-2023-12377357.

Dr. Roberta Lizio was supported by the funds of the project titled "Fast screening of cognitive and motor functions in elderly patients with cognitive-motor deficits using digital indices: a green telemedicine service to reduce the environmental impact of mobility related to the periodic assessment of cognitive functions in healthcare facilities" from the Call PON "Green-digital" resources for technological innovation and environmental sustainability (DM 1062/2021) Program of the Italian Ministry of University and Research.

Prof. Francesco Fontanella was partially supported by the funds of the project "Assessment of brain functions in Lewy Body disease patients using telemonitoring DIGITAL markers as inputs to artificial intelligence (LBDigital)," Call and Sponsor: ANNUAL STRATEGIC PROGRAM OF ITALIAN MINISTRY OF UNIVERSITY AND SCIENTIFIC AND TECHNOLOGICAL RESEARCH, PNRR Mission 4 Component 1 granted by European Union–NextGenerationEU, CUP: B53D23019150006.

Appendix A. Supplementary data

Supplementary data to this article can be found online at https://doi.org/10.1016/j.clinph.2026.2111860.

References

Albert, M.S., DeKosky, S.T., Dickson, D., Dubois, B., Feldman, H.H., Fox, N.C., Gamst, A., Holtzman, D.M., Jagust, W.J., Petersen, R.C., Snyder, P.J., Carrillo, M.C., Thies, B., Phelps, C.H., 2011. The diagnosis of mild cognitive impairment due to Alzheimer's disease: recommendations from the National Institute on Aging-Alzheimer's Association workgroups on diagnostic guidelines for Alzheimer's disease. Alzheimers Dement 7 (3), 270–279. https://doi.org/10.1016/j.jalz.2011.03.008. PMID: 21514249.

Allgaier, J., Mulansky, L., Draelos, R.L., Pryss, R., 2023 Sep. How does the model make predictions? A systematic literature review on the explainability power of machine learning in healthcare. Artif Intell Med 143, 102616. https://doi.org/10.1016/j.artmed.2023.102616. PMID: 37673561.

Almkvist, O., Nordberg, A., 2023 May 2. A biomarker-validated time scale in years of disease progression has identified early- and late-onset subgroups in sporadic Alzheimer's disease. Alzheimers Res Ther 15 (1), 89. https://doi.org/10.1186/s13195-023-01231-8. PMID: 37131241.

Arya, A.D., Verma, S.S., Chakarabarti, P., Chakrabarti, T., Elngar, A.A., Kamali, A.M., Nami, M., 2023. A systematic review on machine learning and deep learning techniques in the effective diagnosis of Alzheimer's disease. Brain Inform 10 (1), 17. https://doi.org/10.1186/s40708-023-00195-7. PMID: 37450224.

Babiloni, C., Arakaki, X., Azami, H., Bennys, K., Blinowska, K., Bonanni, L., Bujan, A., Carrillo, M.C., Cichocki, A., de Frutos-Lucas, J., Del Percio, C., Dubois, B., Edelmayer, R., Egan, G., Epelbaum, S., Escudero, J., Evans, A., Farina, F., Fargo, K., Fernández, A., Ferri, R., Frisoni, G., Hampel, H., Harrington, M.G., Jelic, V., Jeong, J., Jiang, Y., Kaminski, M., Kavcic, V., Kilborn, K., Kumar, S., Lam, A., Lim, L., Lizio, R., Lopez, D., Lopez, S., Lucey, B., Maestú, F., McGeown, W.J., McKeith, I., Moretti, D.V., Nobili, F., Noce, G., Olichney, J., Onofrj, M., Osorio, R., Parra-Rodriguez, M., Rajji, T., Ritter, P., Soricelli, A., Stocchi, F., Tarnanas, I., Taylor, J.P., Teipel, S., Tucci, F., Valdes-Sosa, M., Valdes-Sosa, P., Weiergräber, M., Yener, G., Guntekin, B., 2021a. Measures of resting state EEG rhythms for clinical trials in Alzheimer's disease: Recommendations of an expert panel. Alzheimers Dement 17 (9), 1528–1553. https://doi.org/10.1002/alz.12311. PMID: 33860614.

Babiloni, C., Barry, R.J., Başar, E., Blinowska, K.J., Cichocki, A., Drinkenburg, W.H.I.M., Klimesch, W., Knight, R.T., Lopes da Silva, F., Nunez, P., Oostenveld, R., Jeong, J., Pascual-Marqui, R., Valdes-Sosa, P., Hallett, M., 2020a. International Federation of Clinical Neurophysiology (IFCN) - EEG research workgroup: Recommendations on frequency and topographic analysis of resting state EEG rhythms. Part 1: Applications in clinical research studies. Clin Neurophysiol 131 (1), 285–307. https://doi.org/10.1016/j.clinph.2019.06.234. PMID: 31501011.

Babiloni, C., Benussi, L., Binetti, G., Cassetta, E., Dal Forno, G., Del Percio, C., Ferreri, F., Ferri, R., Frisoni, G., Ghidoni, R., Miniussi, C., Rodriguez, G., Romani, G.L., Squitti, R., Ventriglia, M.C., Rossini, P.M., 2006. Apolipoprotein E and alpha brain rhythms in mild cognitive impairment: a multicentric electroencephalogram study. Ann Neurol 59 (2), 323–334. https://doi.org/10.1002/ana.20724. PMID: 16358334.

Babiloni, C., Blinowska, K., Bonanni, L., Cichocki, A., De Haan, W., Del Percio, C., Dubois, B., Escudero, J., Fernández, A., Frisoni, G., Guntekin, B., Hajos, M., Hampel, H., Ifeachor, E., Kilborn, K., Kumar, S., Johnsen, K., Johannsson, M., Jeong, J., LeBeau, F., Lizio, R., Lopes da Silva, F., Maestú, F., McGeown, W.J., McKeith, I., Moretti, D.V., Nobili, F., Olichney, J., Onofrj, M., Palop, J.J., Rowan, M., Stocchi, F., Struzik, Z.M., Tanila, H., Teipel, S., Taylor, J.P., Weiergräber, M., Yener, G., Young-Pearse, T., Drinkenburg, W.H., Randall, F., 2020b. What electrophysiology tells us about Alzheimer's disease: a window into the synchronization and connectivity of brain neurons. Neurobiol Aging 85, 58–73. https://doi.org/10.1016/j.neurobiolaging.2019.09.008. PMID: 31739167.

Babiloni, C., Del Percio, C., Lizio, R., Marzano, N., Infarinato, F., Soricelli, A., Salvatore, E., Ferri, R., Bonforte, C., Tedeschi, G., Montella, P., Baglieri, A., Rodriguez, G., Famà, F., Nobili, F., Vernieri, F., Ursini, F., Mundi, C., Frisoni, G.B., Rossini, P.M., 2014. Cortical sources of resting state electroencephalographic alpha rhythms deteriorate across time in subjects with amnesic mild cognitive impairment. Neurobiol Aging 35 (1), 130–142. https://doi.org/10.1016/j.neurobiolaging.2013.06.019. PMID: 23906617.

Babiloni, C., Del Percio, C., Lizio, R., Noce, G., Cordone, S., Lopez, S., Soricelli, A., Ferri, R., Pascarelli, M.T., Nobili, F., Arnaldi, D., Aarsland, D., Orzi, F., Buttinelli, C., Giubilei, F., Onofrj, M., Stocchi, F., Stirpe, P., Fuhr, P., Gschwandtner, U., Ransmayr, G., Caravias, G., Garn, H., Sorpresi, F., Pievani, M., Frisoni, G.B., D'Antonio, F., De Lena, C., Güntekin, B., Hanoğlu, L., Başar, E., Yener, G., Emek-Savaş, D.D., Triggiani, A.I., Franciotti, R., De Pandis, M.F., Bonanni, L., 2017. Abnormalities of cortical neural synchronization mechanisms in patients with dementia due to Alzheimer's and Lewy body diseases: an EEG study. Neurobiol Aging 55, 143–158. https://doi.org/10.1016/j.neurobiolaging.2017.03.030. Epub 2017 Apr 5 PMID: 28454845.

Babiloni, C., Del Percio, C., Lizio, R., Noce, G., Lopez, S., Soricelli, A., Ferri, R., Pascarelli, M.T., Catania, V., Nobili, F., Arnaldi, D., Famà, F., Aarsland, D., Orzi, F., Buttinelli, C., Giubilei, F., Onofrj, M., Stocchi, F., Vacca, L., Stirpe, P., Fuhr, P., Gschwandtner, U., Ransmayr, G., Garn, H., Fraioli, L., Pievani, M., Frisoni, G.B., D'Antonio, F., De Lena, C., Güntekin, B., Hanoğlu, L., Başar, E., Yener, G., Emek-Savaş, D.D., Triggiani, A.I., Franciotti, R., Taylor, J.P., De Pandis, M.F., Bonanni, L., 2018. Abnormalities of resting state cortical EEG rhythms in subjects with mild cognitive impairment due to Alzheimer's and Lewy body diseases. J Alzheimers Dis 62 (1), 247–268. https://doi.org/10.3233/JAD-170703. PMID: 29439335.

Babiloni, C., Ferri, R., Noce, G., Lizio, R., Lopez, S., Lorenzo, I., Panzavolta, A., Soricelli, A., Nobili, F., Arnaldi, D., Famà, F., Orzi, F., Buttinelli, C., Giubilei, F., Çipollini, V., Marizzoni, M., Güntekin, B., Aktürk, T., Hanoğlu, L., Yener, G., Özbek, Y., Stocchi, F., Vacca, L., Frisoni, G.B., Del Percio, C., 2021b. Abnormalities of Cortical Sources of Resting State Alpha Electroencephalographic Rhythms are Related to Education Attainment in Cognitively Unimpaired Seniors and Patients with Alzheimer's Disease and Amnesic Mild Cognitive Impairment. Cereb Cortex 31 (4), 2220–2237. https://doi.org/10.1093/cercor/bhaa356. PMID: 33251540.

Babiloni, C., Ferri, R., Noce, G., Lizio, R., Lopez, S., Lorenzo, I., Tucci, F., Soricelli, A., Nobili, F., Arnaldi, D., Famà, F., Orzi, F., Buttinelli, C., Giubilei, F., Cipollini, V., Marizzoni, M., Güntekin, B., Aktürk, T., Hanoğlu, L., Yener, G., Özbek, Y., Stocchi, F., Vacca, L., Frisoni, G.B., Del Percio, C., 2021c. Resting state alpha electroencephalographic rhythms are differently related to aging in cognitively unimpaired seniors and patients with Alzheimer's disease and amnesic mild cognitive impairment. J Alzheimers Dis 82 (3), 1085–1114. https://doi.org/10.3233/JAD-201271. PMID: 34151788.

Babiloni, C., Jakhar, D., Tucci, F., Del Percio, C., Lopez, S., Soricelli, A., Salvatore, M., Ferri, R., Catania, V., Massa, F., Arnaldi, D., Famà, F., Güntekin, B., Yener, G., Stocchi, F., Vacca, L., Marizzoni, M., Giubilei, F., Yıldırım, E., Hanoğlu, L., Hünerli, D., Frisoni, G.B., Noce, G., 2024. Resting state electroencephalographic alpha rhythms are sensitive to Alzheimer's disease mild cognitive impairment progression at a 6-month follow-up. Neurobiol Aging 137, 19–37. https://doi.org/10.1016/j.neurobiolaging.2024.01.013. PMID: 38402780.

Babiloni, C., 2022. The dark side of Alzheimer's disease: neglected physiological biomarkers of brain hyperexcitability and abnormal consciousness level. J Alzheimers Dis 88 (3), 801–807. https://doi.org/10.3233/JAD-220582. PMID: 35754282.

Bishop, C.M., 2006. Pattern recognition and machine learning. Springer-Verlag, Berlin, Heidelberg.

Bonanni, E., Maestri, M., Tognoni, G., Fabbrini, M., Nucciarone, B., Manca, M.L., Gori, S., Iudice, A., Murri, L., 2005. Daytime sleepiness in mild and moderate Alzheimer's disease and its relationship with cognitive impairment. J Sleep Res 14 (3), 311–317. https://doi.org/10.1111/j.1365-2869.2005.00462.x. PMID: 16120107.

Breiman, L., Friedman, H., Olshen, J.A., Stone, C.J., 1984. Classification and regression trees. Wadsworth.

Brown, C.A., Jiang, Y., Smith, C.D., Gold, B.T., 2018. Age and Alzheimer's pathology disrupt default mode network functioning via alterations in white matter microstructure but not hyperintensities. Cortex 104, 58–74. https://doi.org/10.1016/j.cortex.2018.04.006.

Brown, L.M., Schinka, J.A., 2005. Development and initial validation of a 15-item informant version of the geriatric depression scale. Int J Geriatr Psychiatry 20 (10), 911–918. https://doi.org/10.1002/gps.1375.

Brzecka A, Leszek J, Ashraf GM, Ejma M, Ávila-Rodriguez MF, Yarla NS, Tarasov VV, Chubarev VN, Samsonova AN, Barreto GE, Aliev G. Sleep disorders associated with Alzheimer's disease: a perspective. Front Neurosci. 2018;12:330. doi:10.3389/fnins.2018.00330, PMID: 29904334.

Chan, J.Y.C., Liu, J., Chan, A.T.C., Tsoi, K.K.F., 2024. Exergaming and cognitive functions in people with mild cognitive impairment and dementia: a meta-analysis. NPJ Digit Med 7 (1), 154. https://doi.org/10.1038/s41746-024-01142-4. PMID: 38879695.

Chang CC, Lin CJ. LIBSVM: A library for support vector machines. ACM Trans Intell Syst Technol. 2011;2:27:1–27:27. Doi: 10.1145/1961189.1961199.

Cho, H., Choi, J.Y., Lee, S.H., Lee, J.H., Choi, Y.C., Ryu, Y.H., Lee, M.S., Lyoo, C.H., 2017. Excessive tau accumulation in the parieto-occipital cortex characterizes early-onset Alzheimer's disease. Neurobiol Aging 53, 103–111. https://doi.org/10.1016/j.neurobiolaging.2017.01.024. PMID: 28254589.

de Waal, H., Stam, C.J., Blankenstein, M.A., Pijnenburg, Y.A., Scheltens, P., van der Flier, W.M., 2011. EEG abnormalities in early and late onset Alzheimer's disease: understanding heterogeneity. J Neurol Neurosurg Psychiatry 82 (1), 67–71. https://doi.org/10.1136/jnnp.2010.216432. PMID: 20935323.

de Waal, H., Stam, C.J., de Haan, W., van Straaten, E.C., Scheltens, P., van der Flier, W.M., 2012. Young Alzheimer patients show distinct regional changes of oscillatory brain dynamics. Neurobiol Aging 33 (5). https://doi.org/10.1016/j.neurobiolaging.2011.10.013, 1008.e25-31. PMID: 22118944.

Desikan, R.S., Ségonne, F., Fischl, B., Quinn, B.T., Dickerson, B.C., Blacker, D., Buckner, R.L., Dale, A.M., Maguire, R.P., Hyman, B.T., Albert, M.S., Killiany, R.J., 2006. An automated labeling system for subdividing the human cerebral cortex on MRI scans into gyral based regions of interest. Neuroimage. 31 (3), 968–980. https://doi.org/10.1016/j.neuroimage.2006.01.021. PMID: 16530430.

Fischl, B., Salat, D.H., van der Kouwe, A.J., Makris, N., Ségonne, F., Quinn, B.T., Dale, A.M., 2004. Sequence-independent segmentation of magnetic resonance images. Neuroimage 23 (Suppl), 1. https://doi.org/10.1016/j.neuroimage.2004.07.016. PMID: 15501102.

Fletcher, R., 1987. Practical methods of optimization, 2nd ed. John Wiley & Sons, New York, NY. doi: 10.1002/9781118723203.

Folstein, M.F., Folstein, S.E., McHugh, P.R., 1975. "Mini-mental state". A practical method for grading the cognitive state of patients for the clinician. J Psychiatr Res. 12 (3), 189–198. https://doi.org/10.1016/0022-3956(75)90026-6. PMID: 1202204.

Fontanella, F. *et al.* (2022). Machine Learning to Predict Cognitive Decline of Patients with Alzheimer's Disease Using EEG Markers: A Preliminary Study. In: Sclaroff, S., Distante, C., Leo, M., Farinella, G.M., Tombari, F. (eds) Image Analysis and Processing – ICIAP 2022. ICIAP 2022. Lecture Notes in Computer Science, vol 13231. Springer, Cham. Doi: 10.1007/978-3-031-06427-2_12.

Freedman, M., Leach, L., Kaplan, E., Winoucur, G., Shulman, K.J., Delis, D.C., 1994. Clock drawing: a neuropsychological analysis. Oxford University Press, New York.

Friedman, J., Hastie, T., Tibshirani, R., 2000. Additive logistic regression: a statistical view of boosting. Ann Stat 38 (2), 337–374. https://doi.org/10.1214/aos/1016218223.

Frisoni, G.B., Pievani, M., Testa, C., Sabattoli, F., Bresciani, L., Bonetti, M., Beltramello, A., Hayashi, K.M., Toga, A.W., Thompson, P.M., 2007. The topography of grey matter involvement in early and late onset Alzheimer's disease. Brain 130 (Pt 3), 720–730. https://doi.org/10.1093/brain/awl377. PMID: 17293358.

Gouw, A.A., Alsema, A.M., Tijms, B.M., Borta, A., Scheltens, P., Stam, C.J., van der Flier, W.M., 2017. EEG spectral analysis as a putative early prognostic biomarker in nondemented, amyloid positive subjects. Neurobiol Aging 57, 133–142. https://doi.org/10.1016/j.neurobiolaging.2017.05.017. PMID: 28646686.

Grønning, H., Rahmani, A., Gyllenborg, J., Dessau, R.B., Høgh, P., 2012. Does Alzheimer's disease with early onset progress faster than with late onset? A case-control study of clinical progression and cerebrospinal fluid biomarkers. Dement Geriatr Cogn Disord. 33 (2–3), 111–117. https://doi.org/10.1159/000337386. PMID: 22508568.

Huang, C., Wahlund, L., Dierks, T., Julin, P., Winblad, B., Jelic, V., 2000. Discrimination of Alzheimer's disease and mild cognitive impairment by equivalent EEG sources: a cross-sectional and longitudinal study. Clin Neurophysiol 111 (11), 1961–1967. https://doi.org/10.1016/s1388-2457(00)00454-5. PMID: 11068230.

Jack Jr, C.R., Andrews, J.S., Beach, T.G., Buracchio, T., Dunn, B., Graf, A., Hansson, O., Ho, C., Jagust, W., McDade, E., Molinuevo, J.L., Okonkwo, O.C., Pani, L., Rafii, M.S., Scheltens, P., Siemers, E., Snyder, H.M., Sperling, R., Teunissen, C.E., Carrillo, M.C., 2024. Revised criteria for diagnosis and staging of Alzheimer's disease: Alzheimer's Association Workgroup. Alzheimers Dement. https://doi.org/10.1002/alz.13859. PMID: 38934362.

Jack Jr, C.R., Bennett, D.A., Blennow, K., Carrillo, M.C., Dunn, B., Haeberlein, S.B., Holtzman, D.M., Jagust, W., Jessen, F., Karlawish, J., Liu, E., Molinuevo, J.L., Montine, T., Phelps, C., Rankin, K.P., Rowe, C.C., Scheltens, P., Siemers, E., Snyder, H.M., Sperling, R., Contributors, 2018. NIA-AA Research Framework: Toward a biological definition of Alzheimer's disease. Alzheimers Dement. 14 (4), 535–562. https://doi.org/10.1016/j.jalz.2018.02.018. PMID: 29653606.

Jacobs, D., Sano, M., Marder, K., Bell, K., Bylsma, F., Lafleche, G., Albert, M., Brandt, J., Stern, Y., 1994. Age at onset of Alzheimer's disease: relation to pattern of cognitive dysfunction and rate of decline. Neurology 44 (7), 1215–1220. https://doi.org/10.1212/wnl.44.7.1215. PMID: 8035918.

Jeanmonod, D., Magnin, M., Morel, A., 1996. Low-threshold calcium spikes burst in the human thalamus. Common physiopathology for sensory, motor and limbic positive symptoms. Brain 119 (Pt 2), 363–375. https://doi.org/10.1093/brain/119.2.363. PMID: 8800933.

Jelic, V., Johansson, S.E., Almkvist, O., Shigeta, M., Julin, P., Nordberg, A., Winblad, B., Wahlund, L.O., 2000. Quantitative electroencephalography in mild cognitive impairment: longitudinal changes and possible prediction of Alzheimer's disease. Neurobiol Aging 21 (4), 533–540. https://doi.org/10.1016/s0197-4580(00)00153-6. PMID: 10924766.

Jung, W., Jun, E., Suk, H.I., 2021. Alzheimer's Disease Neuroimaging Initiative. Deep recurrent model for individualized prediction of Alzheimer's disease progression. Neuroimage 15 (237), 118143. https://doi.org/10.1016/j.neuroimage.2021.118143. Epub 2021 May 13. PMID: 33991694.

Klimesch, W., Doppelmayr, M., Russegger, H., Pachinger, T., Schwaiger, J., 1998. Induced alpha band power changes in the human EEG and attention. Neurosci Lett 244 (2), 73–76. https://doi.org/10.1016/s0304-3940(98)00122-0. PMID: 9572588.

Klimesch, W., Doppelmayr, M., Russegger, H., Pachinger, T., 1996. Theta band power in the human scalp EEG and the encoding of new information. Neuroreport 7 (7), 1235–1240. https://doi.org/10.1097/00001756-199605170-00002. PMID: 8817539.

Klimesch, W., 1999. EEG alpha and theta oscillations reflect cognitive and memory performance: a review and analysis. Brain Res Brain Res Rev 29 (2–3), 169–195. https://doi.org/10.1016/s0165-0173(98)00056-3. PMID: 10209231.

Klimesch, W., 2012. α-band oscillations, attention, and controlled access to stored information. Trends Cogn Sci 16 (12), 606–617. https://doi.org/10.1016/j.tics.2012.10.007. Epub 2012 Nov 7 PMID: 23141428.

Kluger, A., Gianutsos, J.G., Golomb, J., Ferris, S.H., George, A.E., Franssen, E., Reisberg, B., 1997. Patterns of motor impairement in normal aging, mild cognitive decline, and early Alzheimer's disease. J Gerontol B Psychol Sci Soc Sci 52B (1), P28–P39. https://doi.org/10.1093/geronb/52b.1.p28. PMID: 9008673.

Koric, L., Felician, O., Guedj, E., Hubert, A.M., Mancini, J., Boucraut, J., Ceccaldi, M., 2010. Could clinical profile influence CSF biomarkers in early-onset Alzheimer disease? Alzheimer Dis Assoc Disord. 24 (3), 278–283. https://doi.org/10.1097/WAD.0b013e3181d712d9. PMID: 20473135.

Landis, J.R., Koch, G.G., 1977 Mar. The measurement of observer agreement for categorical data. Biometrics. 33 (1), 159–174. PMID: 843571.

Landwehr, N., Hall, M., Frank, E., 2005. Logistic model trees. Mach Learn 59, 161–205. https://doi.org/10.1007/s10994-005-0466-3.

Lee, J.H., Bliwise, D.L., Ansari, F.P., Goldstein, F.C., Cellar, J.S., Lah, J.J., Levey, A.I., 2007. Daytime sleepiness and functional impairment in Alzheimer disease. Am J Geriatr Psychiatry. 15 (7), 620–626. https://doi.org/10.1097/JGP.0b013e3180381521. PMID: 17586786.

Liang, W., Zhang, K., Cao, P., Liu, X., Yang, J., Zaiane, O., 2021. Rethinking modeling Alzheimer's disease progression from a multi-task learning perspective with deep recurrent neural network. Comput Biol Med 138, 104935. https://doi.org/10.1016/j.neuroimage.2021.118143. PMID: 34656869.

Licht, E.A., McMurtray, A.M., Saul, R.E., Mendez, M.F., 2007. Cognitive differences between early- and late-onset Alzheimer's disease. Am J Alzheimers Dis Other Demen. 22 (3), 218–222. https://doi.org/10.1177/1533317506299156. PMID: 17606531.

Liu, Q., Ganzetti, M., Wenderoth, N., Mantini, D., 2018 Mar. Detecting Large-Scale Brain Networks Using EEG: Impact of Electrode Density, Head Modeling and Source Localization. Front Neuroinform. 2 (12), 4. https://doi.org/10.3389/fninf.2018.00004. PMID: 29551969; PMCID: PMC5841019.

Llinás, R.R., Steriade, M., 2006. Bursting of thalamic neurons and states of vigilance. J Neurophysiol. 95 (6), 3297–3308. https://doi.org/10.1152/jn.00166.2006. PMID: 16554502.

Lopez, S., Hampel, H., Chiesa, P.A., Del Percio, C., Noce, G., Lizio, R., Teipel, S.J., Dyrba, M., González-Escamilla, G., Bakardjian, H., Cavedo, E., Lista, S., Vergallo, A., Lemercier, P., Spinelli, G., Grothe, M.J., Potier, M.C., Stocchi, F., Ferri, R., Habert, M. O., Dubois, B., Babiloni, C., 2024. INSIGHT-preAD study group. The association between posterior resting-state EEG alpha rhythms and functional MRI connectivity in older adults with subjective memory complaint. Neurobiol Aging 137, 62–77. https://doi.org/10.1016/j.neurobiolaging.2024.02.008. PMID: 38431999.

Luckhaus, C., Grass-Kapanke, B., Blaeser, I., Ihl, R., Supprian, T., Winterer, G., Zielasek, J., Brinkmeyer, J., 2008. Quantitative EEG in progressing vs stable mild cognitive impairment (MCI): results of a 1-year follow-up study. Int J Geriatr Psychiatry 23 (11), 1148–1155. https://doi.org/10.1002/gps.2042. PMID: 18537220.

Marino, M., Liu, Q., Brem, S., Wenderoth, N., Mantini, D., 2016. Automated detection and labeling of high-density EEG electrodes from structural MR images. J Neural Eng 13 (5), 056003. https://doi.org/10.1088/1741-2560/13/5/056003. PMID: 27484621.

Marizzoni, M., Ferrari, C., Babiloni, C., Albani, D., Barkhof, F., Cavaliere, L., Didic, M., Forloni, G., Fusco, F., Galluzzi, S., Hensch, T., Jovicich, J., Marra, C., Molinuevo, J. L., Nobili, F., Parnetti, L., Payoux, P., Ranjeva, J.P., Ribaldi, F., Rolandi, E., Rossini, P.M., Salvatore, M., Soricelli, A., Tsolaki, M., Visser, P.J., Wiltfang, J., Richardson, J.C., Bordet, R., Blin, O., Frisoni, G.B., 2020. CSF cutoffs for MCI due to AD depend on APOEε4 carrier status. Neurobiol Aging. 89, 55–62. https://doi.org/10.1016/j.neurobiolaging.2019.12.019. PMID: 32029236.

Marshall, A.C., Cooper, N.R., 2017. The association between high levels of cumulative life stress and aberrant resting state EEG dynamics in old age. Biol Psychol. 127, 64–73. https://doi.org/10.1016/j.biopsycho.2017.05.005. PMID: 28501607.

Mattsson, N., 2011. CSF biomarkers in neurodegenerative diseases. Clin Chem Lab Med. 49 (3), 345–352. https://doi.org/10.1515/CCLM.2011.082. PMID: 21303297.

McGrowder, D.A., Miller, F., Vaz, K., Nwokocha, C., Wilson-Clarke, C., Anderson-Cross, M., Brown, J., Anderson-Jackson, L., Williams, L., Latore, L., Thompson, R., Alexander-Lindo, R., 2021. Cerebrospinal fluid biomarkers of Alzheimer's disease: current evidence and future perspectives. Brain Sci. 11 (2), 215. https://doi.org/10.3390/brainsci11020215. PMID: 33578866.

Meyers, J.L., Zhang, J., Chorlian, D.B., Pandey, A.K., Kamarajan, C., Wang, J.C., Wetherill, L., Lai, D., Chao, M., Chan, G., Kinreich, S., Kapoor, M., Bertelsen, S., McClintick, J., Bauer, L., Hesselbrock, V., Kuperman, S., Kramer, J., Salvatore, J.E., Dick, D.M., Agrawal, A., Foroud, T., Edenberg, H.J., Goate, A., Porjesz, B., 2021. A genome-wide association study of interhemispheric theta EEG coherence: implications for neural connectivity and alcohol use behavior. Mol Psychiatry. 26 (9), 5040–5052. https://doi.org/10.1038/s41380-020-0777-6. PMID: 32433515.

Möller, C., Vrenken, H., Jiskoot, L., Versteeg, A., Barkhof, F., Scheltens, P., van der Flier, W.M., 2013. Different patterns of gray matter atrophy in early- and late-onset Alzheimer's disease. Neurobiol Aging. 34 (8), 2014–2022. https://doi.org/10.1016/j.neurobiolaging.2013.02.013. PMID: 23561509.

Moran, M., Lynch, C.A., Walsh, C., Coen, R., Coakley, D., Lawlor, B.A., 2005. Sleep disturbance in mild to moderate Alzheimer's disease. Sleep Med. 6 (4), 347–352. https://doi.org/10.1016/j.sleep.2004.12.005. PMID: 15978517.

Moretti, D.V., 2015. Conversion of mild cognitive impairment patients in Alzheimer's disease: prognostic value of Alpha3/Alpha2 electroencephalographic rhythms power ratio. Alzheimers Res Ther. 7, 80. https://doi.org/10.1186/s13195-015-0162-x. PMID: 26715588.

Morris, J.C., 1993 Nov. The Clinical Dementia Rating (CDR): current version and scoring rules. Neurology. 43 (11), 2412–2414. https://doi.org/10.1212/wnl.43.11.2412-a. PMID: 8232972.

Niu, X., Wang, Y., Zhang, X., Wang, Y., Shao, W., Chen, L., Yang, Z., Peng, D., 2024. Quantitative electroencephalography (qEEG), apolipoprotein A-I (APOA-I), and apolipoprotein epsilon 4 (APOE ε4) alleles for the diagnosis of mild cognitive impairment and Alzheimer's disease. Neurol Sci. 45 (2), 547–556. https://doi.org/10.1007/s10072-023-07028-9. PMID: 37673807.

Nobili, F., Copello, F., Vitali, P., Prastaro, T., Carozzo, S., Perego, G., Rodriguez, G., 1999. Timing of disease progression by quantitative EEG in Alzheimer's patients. J Clin Neurophysiol. 16 (6), 566–573. https://doi.org/10.1097/00004691-199911000-00008. PMID: 10600024.

Novelli, G., Papagno, C., Capitani, E., Laiacona, M., Vallar, G., Cappa, S.F., 1986. Tre test clinici di ricerca e produzione lessicale. Taratura su soggetti normali. Arch Psicol Neurol Psichiatr. 47, 477–506.

Ossenkoppele, R., Cohn-Sheehy, B.I., La Joie, R., Vogel, J.W., Möller, C., Lehmann, M., van Berckel, B.N., Seeley, W.W., Pijnenburg, Y.A., Gorno-Tempini, M.L., Kramer, J. H., Barkhof, F., Rosen, H.J., van der Flier, W.M., Jagust, W.J., Miller, B.L., Scheltens, P., Rabinovici, G.D., 2015. Atrophy patterns in early clinical stages across distinct phenotypes of Alzheimer's disease. Hum Brain Mapp. 36 (11), 4421–4437. https://doi.org/10.1002/hbm.22927. PMID: 26260856.

Özbek, Y., Fide, E., Yener, G.G., 2021. Resting-state EEG alpha/theta power ratio discriminates early-onset Alzheimer's disease from healthy controls. Clin Neurophysiol. 132 (9), 2019–2031. https://doi.org/10.1016/j.clinph.2021.05.012. PMID: 34284236.

Peter-Derex, L., Yammine, P., Bastuji, H., Croisile, B., 2015. Sleep and Alzheimer's disease. Sleep Med Rev. 19, 29–38. https://doi.org/10.1016/j.smrv.2014.03.007. PMID: 24846773.

Pichet Binette, A., Gonneaud, J., Vogel, J.W., La Joie, R., Rosa-Neto, P., Collins, D.L., Poirier, J., Breitner, J.C.S., Villeneuve, S., Vachon-Presseau, E., 2020. Alzheimer's Disease Neuroimaging Initiative; PREVENT-AD Research Group. Morphometric network differences in ageing versus Alzheimer's disease dementia. Brain. 143 (2), 635–649. https://doi.org/10.1093/brain/awz414. PMID: 32040564.

Pini, L., Geroldi, C., Galluzzi, S., Baruzzi, R., Bertocchi, M., Chitò, E., Orini, S., Romano, M., Cotelli, M., Rosini, S., Magnaldi, S., Morassi, M., Cobelli, M., Bonvicini, C., Archetti, S., Zanetti, O., Frisoni, G.B., Pievani, M., 2020. Age at onset reveals different functional connectivity abnormalities in prodromal Alzheimer's disease. Brain Imaging Behav. 14 (6), 2594–2605. https://doi.org/10.1007/s11682-019-00212-6. PMID: 31903525.

Prichep, L.S., Ghosh Dastidar, S., Jacquin, A., Koppes, W., Miller, J., Radman, T., O'Neil, B., Naunheim, R., Huff, J.S., 2014. Classification algorithms for the identification of structural injury in TBI using brain electrical activity. Comput Biol Med. 53, 125–133. https://doi.org/10.1016/j.compbiomed.2014.07.011. PMID: 25137412.

Prichep, L.S., John, E.R., Ferris, S.H., Rausch, L., Fang, Z., Cancro, R., Torossian, C., Reisberg, B., 2006. Prediction of longitudinal cognitive decline in normal elderly with subjective complaints using electrophysiological imaging. Neurobiol Aging. 27 (3), 471–481. https://doi.org/10.1016/j.neurobiolaging.2005.07.021. PMID: 16213630.

Prichep LS, John ER, Ferris SH, Reisberg B, Almas M, Alper K, Cancro R. Quantitative EEG correlates of cognitive deterioration in the elderly. Neurobiol Aging. 1994;15 (1):85-90. doi:10.1016/0197-4580(94)90147-3. Erratum in: Neurobiol Aging. 1994; 15(3):391. doi: 10.1016/0197-4580(94)90147-3. PMID: 8159266.

Reitan, R.M., 1958. Validity of the Trail Making Test as an indicator of organic brain damage. Percept Mot Skills. 8 (3), 271–276. https://doi.org/10.2466/pms.1958.8.3.271.

Rey, A., 1968. Reattivo della figura complessa. Organizzazioni Speciali, Firenze.

Rhodius-Meester, H.F.M., Benedictus, M.R., Wattjes, M.P., Barkhof, F., Scheltens, P., Muller, M., van der Flier, W.M., 2017. MRI visual ratings of brain atrophy and white matter hyperintensities across the spectrum of cognitive decline are differently affected by age and diagnosis. Front Aging Neurosci. 9, 117. https://doi.org/10.3389/fnagi.2017.00117. PMID: 28536518.

Rijsbergen CJ van. Information retrieval. London: Butterworth-Heinemann; 1979. Doi: 10.1002/asi.4630300621.

Rosen, W.G., Mohs, R.C., Davis, K.L., 1984. A new rating scale for Alzheimer's disease. Am J Psychiatry 141 (11), 1356–1364. https://doi.org/10.1176/ajp.141.11.1356. PMID: 6496779.

Rosen, W.G., Terry, R.D., Fuld, P.A., Katzman, R., Peck, A., 1980 May. Pathological verification of ischemic score in differentiation of dementias. Ann Neurol. 7 (5), 486–488. https://doi.org/10.1002/ana.410070516. PMID: 7396427.

Rossini, P.M., Del Percio, C., Pasqualetti, P., Cassetta, E., Binetti, G., Dal Forno, G., Ferreri, F., Frisoni, G., Chiovenda, P., Miniussi, C., Parisi, L., Tombini, M., Vecchio, F., Babiloni, C., 2006. Conversion from mild cognitive impairment to Alzheimer's disease is predicted by sources and coherence of brain electroencephalography rhythms. Neuroscience 143 (3), 793–803. https://doi.org/10.1016/j.neuroscience.2006.08.049. PMID: 17049178.

Rossini, P.M., Di Iorio, R., Vecchio, F., Anfossi, M., Babiloni, C., Bozzali, M., Bruni, A.C., Cappa, S.F., Escudero, J., Fraga, F.J., Giannakopoulos, P., Guntekin, B., Logroscino, G., Marra, C., Miraglia, F., Panza, F., Tecchio, F., Pascual-Leone, A., Dubois, B., 2020. Early diagnosis of Alzheimer's disease: the role of biomarkers including advanced EEG signal analysis. Report from the IFCN-sponsored panel of experts. Clin Neurophysiol 131 (6), 1287–1310. https://doi.org/10.1016/j.clinph.2020.03.003. PMID: 32302946.

Rossor, M.N., Fox, N.C., Mummery, C.J., Schott, J.M., Warren, J.D., 2010. The diagnosis of young-onset dementia. Lancet Neurol. 9 (8), 793–806. https://doi.org/10.1016/S1474-4422(10)70159-9. PMID: 20650401.

Salinsky, M.C., Oken, B.S., Morehead, L., 1991. Test-retest reliability in EEG frequency analysis. Electroencephalogr Clin Neurophysiol. 79 (5), 382–392. https://doi.org/10.1016/0013-4694(91)90203-g. PMID: 1718711.

Sano, Y., Suzumura, S., Sugioka, J., Mizuguchi, T., Kandori, A., Kondo, I., 2025. Detecting mild cognitive impairment by applying integrated random forest to finger tapping. Med Biol Eng Comput 63 (6), 1881–1894. https://doi.org/10.1007/s11517-025-03306-0. PMID: 39891822.

Seath, P., Macedo-Orrego, L.E., Velayudhan, L., 2023. Clinical characteristics of early-onset versus late-onset Alzheimer's disease: a systematic review and meta-analysis. Int Psychogeriatr 1–17. https://doi.org/10.1017/S1041610223000509. PMID: 37431284.

Stern Y, Gazes Y, Razlighi Q, Steffener J, Habeck C. A task-invariant cognitive reserve network. Neuroimage. 2018 Sep;178:36-45. doi: 10.1016/j.neuroimage.2018.05.033. Epub 2018 May 14. PMID: 29772378; PMCID: PMC6409097.

Subasi A. Use of artificial intelligence in Alzheimer's disease detection. In: Barh D, editor. Artificial intelligence in precision health. Cambridge, MA: Academic Press; 2020. p. 257-78. doi:10.1016/B978-0-12-817133-2.00011-2.

Tsoi, K.K., Chan, J.Y., Hirai, H.W., Wong, S.Y., Kwok, T.C., 2015 Sep. Cognitive Tests to Detect Dementia: A Systematic Review and Meta-analysis. JAMA Intern Med. 175 (9), 1450–1458. https://doi.org/10.1001/jamainternmed.2015.2152. PMID: 26052687.

van der Flier, W.M., Pijnenburg, Y.A., Prins, N., Lemstra, A.W., Bouwman, F.H., Teunissen, C.E., van Berckel, B.N., Stam, C.J., Barkhof, F., Visser, P.J., van Egmond, E., Scheltens, P., 2014. Optimizing patient care and research: the Amsterdam Dementia Cohort. J Alzheimers Dis 41 (1), 313–327. https://doi.org/10.3233/JAD-132306. PMID: 24614907.

van der Vlies, A.E., Koedam, E.L., Pijnenburg, Y.A., Twisk, J.W., Scheltens, P., van der Flier, W.M., 2009. Most rapid cognitive decline in APOE epsilon4 negative Alzheimer's disease with early onset. Psychol Med 39 (11), 1907–1911. https://doi.org/10.1017/S0033291709005492. PMID: 19335933.

Wallin, A.K., Blennow, K., Zetterberg, H., Londos, E., Minthon, L., Hansson, O., 2010. CSF biomarkers predict a more malignant outcome in Alzheimer disease. Neurology. 74 (19), 1531–1537. https://doi.org/10.1212/WNL.0b013e3181dd4dd8. PMID: 20458070.

Wang, S.H., Zhang, Y., Li, Y.J., 2018. Single slice-based detection for Alzheimer's disease via wavelet entropy and multilayer perceptron trained by biogeography-based optimization. Multimed Tools Appl. 77, 10393–10417. https://doi.org/10.1007/s11042-016-4222-4.

Wattmo, C., Wallin, Å.K., 2017. Early- versus late-onset Alzheimer's disease in clinical practice: cognitive and global outcomes over 3 years. Alzheimers Res Ther 9 (1), 70. https://doi.org/10.1186/s13195-017-0294-2. PMID: 28859660.

Wechsler, D., 1987. Manual for the Wechsler Memory Scale-Revised. The Psychological Corporation, San Antonio, TX.

Wilson, R.S., Gilley, D.W., Bennett, D.A., Beckett, L.A., Evans, D.A., 2000. Person-specific paths of cognitive decline in Alzheimer's disease and their relation to age. Psychol Aging 15 (1), 18–28. https://doi.org/10.1037//0882-7974.15.1.18. PMID: 10755286.

Yu, H., Huang, F., Lin, C., 2011. Dual coordinate descent methods for logistic regression and maximum entropy models. Mach Learn 85 (1–2), 41–75. https://doi.org/10.1007/s10994-010-5221-8.

Zou, K.H., O'Malley, A.J., Mauri, L., 2007. Receiver-operating characteristic analysis for evaluating diagnostic tests and predictive models. Circulation 115 (5), 654–657. https://doi.org/10.1161/CIRCULATIONAHA.105.594929. PMID: 17283280.